

**PARALLEL POLYMER-BASED MICROEXTRACTION METHODS TO STUDY  
INTERMOLECULAR ASSOCIATION AND PHYSICOCHEMICAL PROPERTIES**

by

**Dujuan Lu**

Bachelor of Science, Nanjing University, 2006

Submitted to the Graduate Faculty of the  
Kenneth P. Dietrich School of Arts and Sciences in partial fulfillment  
of the requirements for the degree of  
Doctor of Philosophy

University of Pittsburgh

2014

UNIVERSITY OF PITTSBURGH  
THE KENNETH P. DIETRICH SCHOOL OF ARTS AND SCIENCES

This dissertation was presented

by

Dujuan Lu

It was defended on

July 8<sup>th</sup>, 2014

and approved by

Alexander Star, Professor, Department of Chemistry

Adrian C. Michael, Professor, Department of Chemistry

Xiang-Qun Xie, Professor, Department of Pharmaceutical Sciences

Dissertation Advisor: Stephen G. Weber, Professor, Department of Chemistry

Copyright © by Dajuan Lu

2014

# **PARALLEL POLYMER-BASED MICROEXTRACTION METHODS TO STUDY INTERMOLECULAR ASSOCIATION AND PHYSICOCHEMICAL PROPERTIES**

Dujuan Lu, PhD

University of Pittsburgh, 2014

Lipophilicity and acid dissociation constants are important physicochemical properties that in part determine the suitability of an organic molecule as a pharmacological agent. Intermolecular associations are omnipresent in chemical and biochemical systems and particularly important in the efficacy of an excipient for a poorly soluble drug. Current standard methods to determine lipophilicity require large amounts of pure sample and have problems due to emulsion formation. This dissertation describes a method based on distribution of the solutes between a polymer phase and an aqueous phase in a 96-well format, in the presence and absence of a receptor (e.g., candidate excipient) in one of the two phases. This parallel approach uses minimal amounts of organic solvent and only requires small amounts of sample. This approach has been used to determine polymer-water distribution coefficients of solutes. In addition, by measuring polymer-water distribution coefficients at a variety of experimental conditions, such as pH and receptor concentration, acid dissociation constants and solute-receptor binding constants have been successfully determined for several chemical systems.

This method has been applied to measure binding constants of econazole with six cyclodextrins in aqueous solutions. The acid dissociation constant of econazole was determined by measuring econazole-cyclodextrin binding constants at various pH values. Distribution coefficients and acid dissociation constants of twenty-four novel drug-like compounds have also been determined by this parallel approach and compared to the values calculated by

commercially available software. The software packages did not adequately predict experimental results, especially for ionizable compounds. This emphasizes the need for laboratory separations-based measurements of distribution coefficients. The polymeric phase was poly(vinyl chloride) (PVC) plasticized by 67% (w/w) dioctyl sebacate (DOS). Intermolecular association has also been studied in Teflon AF 2400, a fluorinated polymer phase, with and without fluorinated hydrogen bond donor Krytox 157 FSH in the 96-well approach. In addition, a novel fluorinated receptor-doped fiber solid phase microextraction (SPME) was developed to selectively detect quinoline in aqueous solutions.

## TABLE OF CONTENTS

|   |             |
|---|-------------|
| <b>PREFACE.....</b>   | <b>XIII</b> |
| <b>1.0 INTRODUCTION.....</b>  | <b>1</b>    |
| <b>1.1 SOLID PHASE MICROEXTRACTION .....</b>  | <b>1</b>    |
| <b>1.1.1 Introduction .....</b>   | <b>1</b>    |
| <b>1.1.2 SPME theories: from distribution to kinetics .....</b>   | <b>3</b>    |
| <b>1.1.3 Receptor-doped polymer coating materials as SPME sorbents .....</b>  | <b>9</b>    |
| <b>1.1.4 Parallel design and automation of SPME.....</b>  | <b>11</b>   |
| <b>1.2 METHODS FOR MEASUREMENT OF ACID DISSOCIATION<br/>CONSTANT .....</b>  | <b>13</b>   |
| <b>1.3 METHODS FOR LIPOPHILICITY MEASUREMENT .....</b>  | <b>15</b>   |
| <b>1.4 OUTLINE.....</b>   | <b>16</b>   |
| <b>2.0 DETERMINATION OF DRUG-CYCLODEXTRIN BINDING CONSTANTS<br/>BY A HIGH-THROUGHPUT PHASE-DISTRIBUTION METHOD.....</b> | <b>20</b>   |
| <b>2.1 INTRODUCTION .....</b>   | <b>20</b>   |
| <b>2.2 EXPERIMENTAL.....</b>  | <b>23</b>   |
| <b>2.2.1 Materials.....</b>   | <b>23</b>   |
| <b>2.2.2 Equipment .....</b>  | <b>23</b>   |
| <b>2.2.3 Buffer Preparation .....</b>   | <b>24</b>   |

|       |   |    |
|-------|---|----|
| 2.2.4 | Preparation of Plasticized PVC Films .....  | 24 |
| 2.2.5 | High-Throughput Phase-Distribution Studies.....   | 24 |
| 2.2.6 | HPLC Method to Determine Econazole Concentration .....  | 26 |
| 2.2.7 | DOS binding to CDs. ....  | 26 |
| 2.3   | RESULTS AND DISCUSSION .....  | 26 |
| 2.3.1 | Theories to Determine the Stoichiometry $n$ and Binding Constants $K_{1:i}$ ( $i = 1$ to $n$ )..... | 26 |
| 2.3.2 | Experimental Results and Discussion .....   | 30 |
| 2.4   | CONCLUSIONS .....   | 40 |
| 3.0   | LIPOPHILICITY SCREENING OF NOVEL DRUG-LIKE COMPOUNDS AND<br>COMPARISON TO $CLOGP$ .....             | 42 |
| 3.1   | INTRODUCTION .....  | 42 |
| 3.2   | EXPERIMENTAL.....   | 45 |
| 3.2.1 | Materials.....  | 45 |
| 3.2.2 | Equipment .....   | 49 |
| 3.2.3 | Buffer Preparation .....  | 49 |
| 3.2.4 | Determination of $\log P_{pw}$ and $pK_a$ of a Solute.....  | 50 |
| 3.2.5 | UHPLC Method to Determine Concentrations of the Thiadiazine .....                                   | 52 |
| 3.2.6 | UV Plate Reader Method to Determine Concentrations of the Thiadiazine<br>.....                      | 52 |
| 3.2.7 | Lipophilicity Screening of the Library .....  | 52 |
| 3.3   | RESULTS AND DISCUSSION .....  | 53 |

|       |  |    |
|-------|--|----|
| 3.3.1 | Theories to Determine Partition Coefficient and $pK_a$ of a Solute simultaneously .....    | 53 |
| 3.3.2 | Determination of $\log P_{pw}$ and $pK_a$ of a solute in a 96-well format .....            | 54 |
| 3.3.3 | Optical Absorbance-based Lipophilicity Screening of a Library of Drug-like Compounds ..... | 58 |
| 3.4   | CONCLUSIONS .....  | 63 |
| 4.0   | FLUOROUS RECEPTOR-FACILITATED SOLID PHASE MICROEXTRACTION .....                            | 65 |
| 4.1   | INTRODUCTION .....   | 65 |
| 4.2   | EXPERIMENTAL .....   | 69 |
| 4.2.1 | Chemicals and Solutions .....  | 69 |
| 4.2.2 | 96-well Vessel SPME: Preparation and Extraction .....                                      | 70 |
| 4.2.3 | Coated Fiber SPME-GC: Fiber Preparation, Extractions, and Desorption on GC .....           | 72 |
| 4.3   | RESULTS AND DISCUSSION .....   | 74 |
| 4.3.1 | 96-well Vessel SPME .....  | 74 |
| 4.3.2 | Coated Fiber SPME .....  | 81 |
| 4.4   | CONCLUSIONS .....  | 85 |
|       | BIBLIOGRAPHY .....   | 86 |

## LIST OF TABLES

|   |    |
|---|----|
| Table 2.1 Binding constants of econazole with six CDs .....   | 33 |
| Table 2.2 Binding constants of econazole with HP- $\beta$ -CD at various temperatures.....  | 34 |
| Table 3.1 Experimental Design of 24 compounds in a 96-well microplate.....  | 47 |
| Table 3.2 PubChem SID of 24 compounds in a 96-well microplate .....   | 48 |
| Table 3.3 Experimental and calculated log <i>D</i> results for 24 compounds at pH 4.0, 7.0, 10.0.....                                 | 60 |
| Table 3.4 Experimental and calculated log <i>P</i> results for 10 neutral compounds in the library. ...                               | 62 |
| Table 4.1 Distribution coefficients and selectivity for quinoline and phenol in pure Teflon AF<br>and Teflon AF with 50% Krytox ..... | 80 |

## LIST OF FIGURES

|  |    |
|--|----|
| Figure 1.1 Various configurations of SPME. The red color describes the extraction phase, which can be coated on a fiber, or inside the wall and bottom of a vessel, depending on the configuration. Reproduced with permission from reference[3]. Copyright (2011) American Chemical Society. ....   | 3  |
| Figure 1.2 Typical extraction time profile of SPME. Reprinted with permission from reference[5]. Copyright (2007) Elsevier. ....   | 8  |
| Figure 1.3 SPME device and operation. (1) Place rod in sample solution for a designated time. (2) Injection 5 $\mu$ L of back extraction solution into the Teflon tube. (3) Remove rod, wipe clean, place in Teflon tube. (4) Remove after a set time (5) Collect the solution by moving the droplet spanning the diameter as a piston and transfer the drop to an injection vial. Reprinted with permission from reference[29]. Copyright (1997) American Chemical Society..... | 11 |
| Figure 1.4 (a) 96-well multi-fiber SPME device (stainless steel fibers coated with carbon tape). (b) robot arm inserting the multi-fiber SPME device in the 96-well plate. Reprinted with permission from reference[32]. Copyright (2008) Elsevier.....  | 13 |
| Figure 1.5 General procedure of the parallel experimental design to study intermolecular association and physicochemical properties .....  | 19 |
| Figure 2.1 Structure of econazole .....  | 22 |

|   |    |
|---|----|
| Figure 2.2 Schematic illustration of the preparation and use of polymer films in 96-well plates   | 25 |
| Figure 2.3 Percentage of econazole extracted as a function of time in the presence of six CDs and without CD.....                                     | 30 |
| Figure 2.4 Effect of CD concentrations on econazole equilibrium concentration in the aqueous phase .....  | 32 |
| Figure 2.5 Multivariate linear regression results for fitting $D/D_0$ versus CD concentration. ....   | 33 |
| Figure 2.6 van't Hoff plot for econazole - HP- $\beta$ -CD complex .....  | 35 |
| Figure 2.7 Effect of pH on the apparent binding constant of the econazole-HP- $\beta$ -CD complex .   | 38 |
| Figure 3.1 Chemical structure of 2H-1, 2, 6-thiadiazine, 3-methyl-5-phenyl-, 1, 1-dioxide.....  | 45 |
| Figure 3.2 Schematic of the preparation and use of polymer films in 96-well plates for $\text{Log } D_{pw}$ determination. ....                       | 51 |
| Figure 3.3 Distribution coefficients of 2H-1, 2, 6-thiadiazine, 3-methyl-5-phenyl-, 1, 1-dioxide at various pH values analyzed by UHPLC. ....         | 55 |
| Figure 3.4 Distribution coefficients of 2H-1, 2, 6-thiadiazine, 3-methyl-5-phenyl-, 1, 1-dioxide at various pH values determined by plate reader..... | 56 |
| Figure 3.5 Correlation of distribution coefficients between different runs. ....  | 58 |
| Figure 3.6 Correlation of distribution coefficients between our experimental values and calculated values. ....                                       | 61 |
| Figure 4.1 Structure of Ktytox 157 FSH (1), Teflon AF 2400 (2), quinoline (3).....  | 68 |
| Figure 4.2 General procedure for 96-well vessel SPME. ....  | 70 |
| Figure 4.3 Percentage of quinoline extracted as a function of time for Teflon AF films with different percentages of receptor doped.....              | 74 |

|   |    |
|---|----|
| Figure 4.4 Log $D_{pw}$ of quinoline as a function of Krytox concentration in Teflon AF films for quinoline with an initial aqueous concentration of 50 $\mu\text{M}$ . ..... | 75 |
| Figure 4.5 Polymer-water distribution coefficient of quinoline as a function of the initial quinoline aqueous concentration.....  | 79 |
| Figure 4.6 Quinoline amount extracted in both liquid phase and headspace as a function of quinoline initial concentration. ....   | 82 |
| Figure 4.7 Kinetic profile of extracted quinoline amount by the coated fiber (50% Krytox in Teflon AF) SPME-GC at different headspace exposure times. ....                    | 84 |

## PREFACE

I would like to take this opportunity to thank people who have contributed to my success in completing this dissertation.

First and foremost, I would like to thank my research advisor, Prof. Stephen G. Weber. He is an excellent scientist and a wonderful teacher. He taught me how to be an independent researcher. With his solid knowledge of science, he has always provided me with useful guidance and valuable advice.

I am also thankful to my committee members, who have also guided me over the years. Prof. Alex Star is also the committee member of my comprehensive exam and the mentor of my research proposal. I have learnt a lot from him through our discussions. Prof. Adrian Michael, who is also the committee member of my comprehensive exam and research proposal, has given me a lot of great advice especially in the analytical field. I also thank them and Prof. Xiang-Qun Xie for giving their valuable time to serve as my dissertation committee members.

I was lucky to work with a number of excellent collaborators. I would like to thank Prof. Peter Wipf, Pete Chambers, Prof. Xiang-Qun Xie, and other members within the University of Pittsburgh Center for Chemical Methodologies and Library Development (UPCMLD). UPCMLD weekly meetings have given me valuable opportunities for public presentations, discussion and collaboration with scientists from various fields.

I am also thankful to members of my research group for their helpful discussions and kind spirits, especially Dr. Zhi Chen, Dr. Hui Fang, Dr. Kristi Kauffman, Dr. Hong Zhang, Dr. Yanhong Yang, Candace McGowan, Sijia Wang and Yangguang Ou.

Last but not the least; I am eternally indebted to my family. Although my parents cannot understand my dissertation, they always support me to pursue my PhD dream and encourage me when I feel frustrated. I am also especially grateful to my beloved husband, Xing Yin, who has been together with me since college. He has played many roles in my life, as my lover, as my best friend, and as a fellow chemist I can discuss science with. I cannot thank him enough for his love and support through all these years.

## **1.0 INTRODUCTION**

### **1.1 SOLID PHASE MICROEXTRACTION**

#### **1.1.1 Introduction**

Sample preparation methods have been developed to clean up the sample matrix and preconcentrate target analytes to enhance the measurement signal. Sample preparation is an essential step in the analysis process. Over 60% of the total analysis time is spent on preparing samples before introducing them into analytical instruments[1]. The success of an analysis of samples with a complex matrix also depends on those sample preparation steps. It is necessary to develop fast, efficient, and environmentally friendly procedures.

Extractions are the most commonly used sample preparation techniques. Extraction is a separation process to remove target analytes from a sample matrix. According to the nature of the extraction phase, extraction methods can be classified into liquid phase extraction (LPE) and solid phase extraction (SPE). Liquid-liquid extraction (LLE) is a widely used method to separate compounds based on their distribution between two immiscible liquid phases. This method is time consuming and labor intensive, has problems of emulsion formation, and consumes large amounts of volatile organic solvents.

A growing concern for protecting the environment has led to an increased emphasis on green analytical methods. Solvent-free systems are ideal for preventing hazards to the environment and human health. SPE was originally developed as a solvent-free alternative to LLE. In SPE, analytes are removed from a flowing sample matrix through sorption to a solid phase, which is usually a polymer. A wash solution is chosen to desorb analytes of interest. Compared to LLE, SPE has several advantages: high recovery and reproducibility, high efficiency with regard to economy of time and labor, and reduction in the amount of organic solvents used.

Solid phase microextraction (SPME) is a solvent-free extraction technique in which the extraction medium is small, usually on a coated fiber or thin film. The process of SPME involves two main steps: (1) extraction of the target analyte from the sample matrix to the polymer sorbent and (2) desorption of the concentrated analytes from the sorbent to an instrument for analysis[2]. Various configurations of SPME have been considered to date, including coated fibers, vessels, stirrers, and membranes as illustrated in Figure 1.1[3].

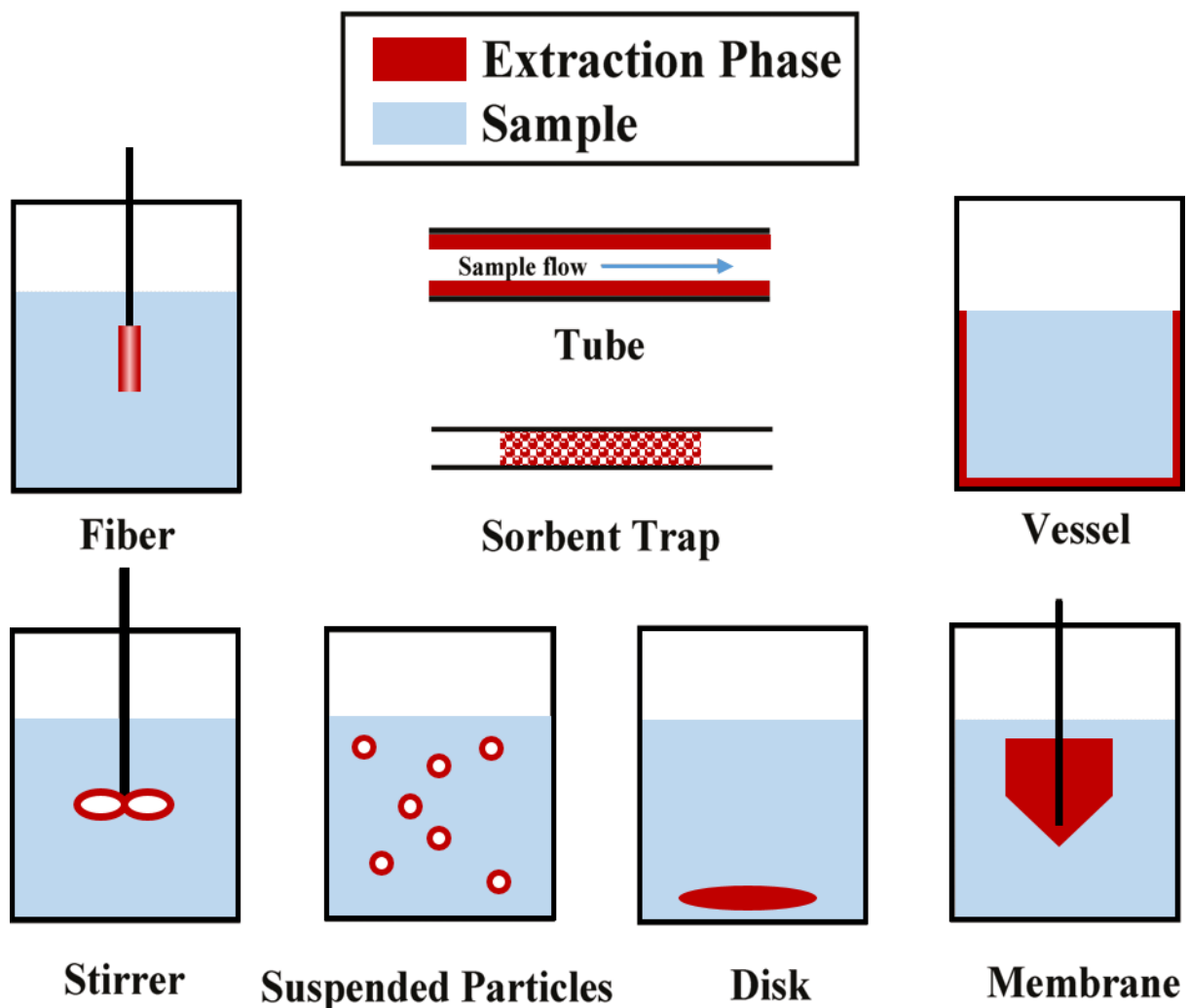


Figure 1.1 Various configurations of SPME. The red color describes the extraction phase, which can be coated on a fiber, or inside the wall and bottom of a vessel, depending on the configuration. Reproduced with permission from reference[3]. Copyright (2011) American Chemical Society.

### 1.1.2 SPME theories: from distribution to kinetics

Both distribution coefficient ( $D$ ) and partition coefficient ( $P$ ) between the polymer phase and the aqueous phase can be used to describe extraction efficiency of SPME. They are defined as the ratio of equilibrium concentrations ( $C$ ) of an analyte in two immiscible phases. However,

there is a clear distinction between those two concepts. Partition coefficient (P) reflects the concentration ratio of the neutral species only, while the distribution coefficient (D) counts for both neutral and ionized species.

For ionizable compounds, D should be used instead of P in the pH range where ionic species exist. In practice not only neutral molecules but also ion pairs may partition. The distribution of the neutral and ionized forms of the solute between the polymer film phase and the aqueous phase is determined by the distribution coefficient  $D_{pw}$ :

$$D_{pw} = \frac{[S^-]_f + [S]_f}{[S^-]_{Aq} + [S]_{Aq}} \quad \text{Equation 1.1}$$

where  $[S]_{Aq}$  and  $[S]_f$  are the concentrations of the neutral solute in the aqueous phase and film phase, respectively;  $[S^-]_{Aq}$  and  $[S^-]_f$  are the concentrations of the ionized solute and its ion pair in the aqueous phase and film phase, respectively.

The partition coefficient (P) for the neutral form of the solute is defined as:

$$P_{pw} = \frac{[S]_f}{[S]_{Aq}} \quad \text{Equation 1.2}$$

The conditional partition coefficient for the anionic solute in the presence of a particular set of counterions at certain concentrations is defined as:

$$P_{pw}^- = \frac{[S^-]_f}{[S^-]_{Aq}} \quad \text{Equation 1.3}$$

It is known that the equilibrium equation for acid dissociation constant  $K_a$  is

$$K_a = \frac{[S^-]_{Aq} [H^+]}{[S]_{Aq}} \quad \text{Equation 1.4}$$

Inserting Equation (1.2), (1.3), and (1.4) into Equation (1.1), yields:

$$D_{pw} = \frac{P_{pw} + P_{pw}^- \cdot \frac{[S^-]_{Aq}}{[S]_{Aq}}}{1 + \frac{[S^-]_{Aq}}{[S]_{Aq}}} = \frac{P_{pw} + P_{pw}^- \cdot \frac{K_a}{[H^+]}}{1 + \frac{K_a}{[H^+]}} = P_{pw}^- + \frac{P_{pw} - P_{pw}^-}{1 + 10^{pH - pK_a}} \quad \text{Equation 1.5}$$

By plotting  $D_{pw}$  versus pH, the  $P_{pw}$ ,  $P_{pw}^-$  and  $pK_a$  values of the ionizable solute can be obtained by applying a nonlinear least-squares curve fitting according to Equation (1.5). When only single neutral species exists, partition coefficient (P) and distribution coefficient (D) are identical.

Coated fiber SPME is the most widely used SPME configuration. It is performed by either direct or headspace extraction. In the direct extraction mode, the coated fiber is inserted into the sample matrix to extract analytes into the extraction phase. In the headspace extraction mode, the fiber is inserted into the gaseous headspace above the sample matrix to extract relatively volatile analytes. Headspace SPME is a multiphase distribution process that includes three phases: sample matrix, the gaseous headspace, and the fiber coating. During the extraction, analytes partition between all three phases. Direct extraction can be considered as a simpler case (no headspace) of three phase distribution. It is important to understand the distribution and mass transfer processes of the extraction.

The amount of an analyte extracted by the polymeric coating is related to the overall distribution of the analyte in the multiphase system. The total mass of an analyte remains constant during the extraction:

$$C_0V_s = C_fV_f + C_hV_h + C_sV_s \quad \text{Equation 1.6}$$

where  $C_0$  is the initial concentration of the analyte in the sample matrix,  $C_f$ ,  $C_h$ , and  $C_s$  are the concentrations of the analyte in the polymeric fiber coating, the headspace and the sample, respectively, and  $V_f$ ,  $V_h$  and  $V_s$ , are the volumes of the polymeric fiber coating, the headspace, and the sample, respectively. Note that here we assume only single neutral species is present in

each phase to simplify the discussion. In most applications, the experimental conditions can be tuned so that the neutral species dominates.

The film-headspace partition coefficient  $P_{fh}$  is then defined as:

$$P_{fh} = \frac{C_f}{C_h} \quad \text{Equation 1.7}$$

The headspace-solution partition coefficient  $P_{hs}$  is defined as:

$$P_{hs} = \frac{C_h}{C_s} \quad \text{Equation 1.8}$$

Thus, the film-solution partition coefficient  $P_{fs}$  is described as:

$$P_{fs} = P_{fh} \cdot P_{hs} \quad \text{Equation 1.9}$$

The amount of analyte extracted  $n$  is defined as:

$$n = C_f V_f \quad \text{Equation 1.10}$$

Combing Equation (1.7), (1.8), (1.9), and (1.10), yields:

$$n = \frac{P_{fs} V_f V_s C_0}{P_{fs} V_f + P_{hs} V_h + V_s} \quad \text{Equation 1.11}$$

where  $P_{fs}$  is the partition coefficient of the analyte between the fiber coating and the sample matrix. If there is no headspace in the sample vial (direct liquid extraction), the term  $P_{hs}V_h$  in the denominator can be eliminated, resulting in:

$$n = \frac{P_{fs} V_f V_s C_0}{P_{fs} V_f + V_s} \quad \text{Equation 1.12}$$

For large sample volumes, when  $P_{fs}V_f \ll V_s$ , Equation (1.12) can be simplified to

$$n = P_{fs} V_f C_0 \quad \text{Equation 1.13}$$

The above equations show that the amount of the analyte extracted depends on its partition coefficient between the sample matrix and the sorbent phase, the volumes of the extraction phase and sample matrix, and the initial concentration.

The partition coefficients between the extraction phase and the sample matrix depend on a variety of conditions, including temperature, pressure, and exact matrix composition. Temperature effects need to be considered when temperature changes during the extraction procedure. When the temperatures of both the fiber and sample matrix change from  $T_0$  to  $T$ , the partition coefficient changes according to the following equation (assuming the changes in entropy and enthalpy are independent of temperature)[4]:

$$P_{fs} = P_0 \exp \left[ -\frac{\Delta H^o}{R} \left( \frac{1}{T} - \frac{1}{T_0} \right) \right] \quad \text{Equation 1.14}$$

where  $P_0$  is the partition coefficient at temperature  $T_0$ ,  $\Delta H^o$  is the molar enthalpy change of the analyte from the sample matrix to fiber coating, and  $R$  is the gas constant.

Figure 1.2 shows a typical SPME extraction kinetics profile. There is a quick increase in the extracted amount of analyte right after the contact of the fiber with the sample. The rate then decreases and equilibrium is eventually achieved. The profile is approximately linear in the beginning of the kinetic process.

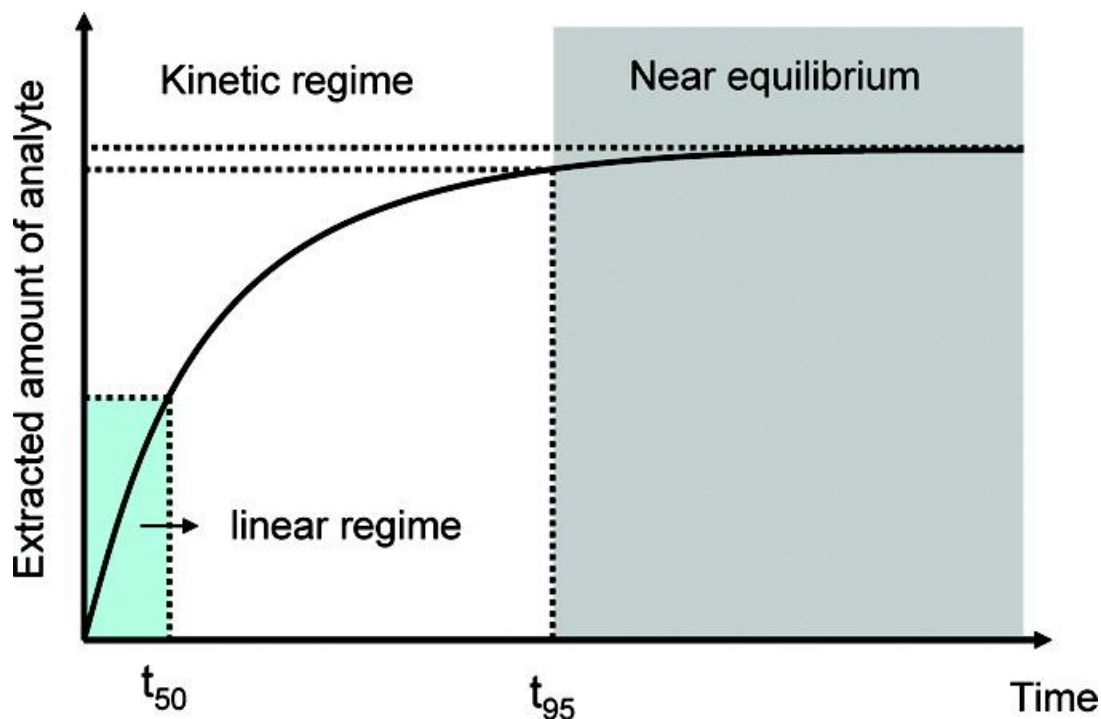


Figure 1.2 Typical extraction time profile of SPME. Reprinted with permission from reference[5].

Copyright (2007) Elsevier.

The use of the headspace (HS) extraction speeds up the extraction process. For volatile compounds, a big portion of the analyte is already in the headspace before the extraction. Diffusion coefficients are usually 4-5 orders of magnitude larger in the gas phase than in the liquid phase[3]. Therefore, HS-SPME results in faster equilibration than liquid-phase SPME (direct liquid extraction).

The kinetics of analyte from the sample matrix into a SPME coating for large sample volumes can be described by [6,7]:

$$n = [1 - \exp(-a \cdot t)] \cdot P_{fs} \cdot V_f \cdot C_0 \quad \text{Equation 1.15}$$

where  $n$  is the amount of analyte extracted,  $P_{fs}$  is the partition coefficient of the analyte between the fiber coating and the sample matrix,  $V_f$  is the volume of extraction phase, and  $C_0$  is the initial concentration of the analyte,  $t$  is the exposure time,  $a$  is a parameter measuring how fast equilibrium can be reached, which is a constant for a constantly agitated system. The amount of

analyte extracted is proportional to the initial analyte concentration once the sampling time and agitation conditions are held constant. Therefore, the quantitative analysis of SPME is feasible before partition equilibrium is reached.

### **1.1.3 Receptor-doped polymer coating materials as SPME sorbents**

The selection of polymer coating material is the most important step in controlling the selectivity of the extraction[8]. The most common fiber materials are polydimethylsiloxane (PDMS), divinylbenzene (DVB), polyacrylate (PA), Carboxen (CAR; a carbon molecular sieve) and Carbowax (CW; polyethylene glycol). Coatings of blended materials are also available, such as PDMS-DVB, PDMS-CAR, CW-DVB[9]. However, there is no universal sorbent for all applications.

One of the recent trends in SPME is to study new coatings with higher extraction efficiency and selectivity[9]. The recently developed coatings for selective extraction include molecularly imprinted polymer[10-18], ionic liquid[19-23], metal complex[24], and carbon nanotubes[25,26].

Receptors are potentially very powerful tools for selective extractions by taking advantage of a specific interaction between a receptor and a substrate through noncovalent bonding, such as hydrogen bonding, metal coordination,  $\pi$ - $\pi$  interactions, hydrophobic forces, van der Waals, electrostatic effects, and steric effects[27].

When a receptor is present either in the polymer phase or in the aqueous phase, the stoichiometry and binding constant of solute-receptor complexation can be determined by measuring distribution coefficient of the solute at various receptor concentrations. If a receptor is

added into the polymer film phase, solute and receptor forms a complex and the binding constant is defined as:

$$K_{1:n} = \frac{[S \cdot L_n]_f}{[S]_f [L]_f^n} \quad \text{Equation 1.16}$$

where  $n$  is the stoichiometry,  $[L]_f$  is the free receptor concentration and  $[S \cdot L_n]_f$  is the solute-receptor complex concentration in the polymer phase. The apparent solute distribution coefficient  $D_{app}$  with the presence of a receptor in the polymer phase is:

$$D_{app} = \frac{[S]_f + [S \cdot L_n]_f}{[S]_{aq}} \quad \text{Equation 1.17}$$

Dividing Equation (1.17) by Equation (1.2):

$$\frac{D_{app}}{P_{pw}} = 1 + \frac{[S \cdot L_n]_f}{[S]_f} \quad \text{Equation 1.18}$$

After rearranging Equation (1.18) and inserting it into Equation (1.16), we obtain:

$$K_{1:n} = \frac{[S \cdot L_n]_f}{[S]_f [L]_f^n} = \left( \frac{D_{app}}{P_{pw}} - 1 \right) \cdot \frac{1}{[L]_f^n} \quad \text{Equation 1.19}$$

After converting Equation (1.19) into the logarithmic form and rearranging it, we get

$$\log \left( \frac{D_{app}}{P_{pw}} - 1 \right) = \log K_{1:n} + n \cdot \log [L]_f \quad \text{Equation 1.20}$$

The stoichiometry  $n$  and binding constant  $K_{1:n}$  can be determined by measuring distribution coefficient as a function of receptor concentration.

Our group has done a great deal of work combining molecular recognition processes with separation and sample preparation methods. Li and coworkers[28] have reported an SPME device based on plasticized-poly (vinyl chloride) (PVC) extraction medium coupled with molecular recognition. They incorporated a phenobarbital receptor into a plasticized PVC film

coated on a primed steel rod and followed the sampling with micro back-extraction for capillary electrophoresis-based determination as shown in Figure 1.3. Such receptors are potentially very powerful tools for selective extractions by taking advantage of noncovalent bonding between a receptor and an analyte.

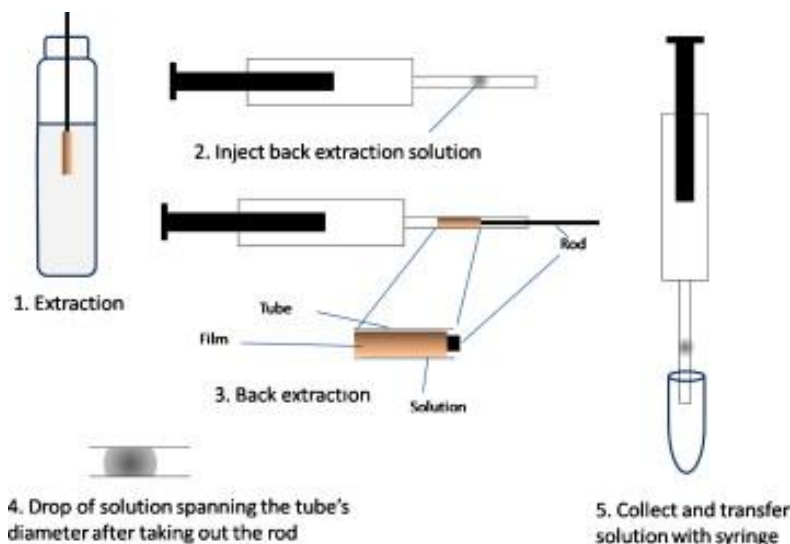


**Figure 1.3 SPME device and operation. (1) Place rod in sample solution for a designated time. (2) Injection 5  $\mu\text{L}$  of back extraction solution into the Teflon tube. (3) Remove rod, wipe clean, place in Teflon tube. (4) Remove after a set time (5) Collect the solution by moving the droplet spanning the diameter as a piston and transfer the drop to an injection vial. Reprinted with permission from reference[29]. Copyright (1997) American Chemical Society.**

#### **1.1.4 Parallel design and automation of SPME**

High-throughput screening (HTS) has recently become a hot method for scientific experimentation. The key testing vessel of HTS is the microplate: a small, usually disposable, plastic container that features a grid of small wells. Modern microplates for HTS generally have 96, 384, or other multiples of 96 wells. Automation is another important characteristic. HTS is a relatively recent innovation, made available through modern advances in robotics and high-speed

instruments. Since 1990, pharmaceutical and biotechnology companies have gradually moved toward HTS of small-molecule compounds for their discovery programs[30].

The automation of SPME in parallel format allows significant reduction in analysis time and increase in sample throughput. The automation of SPME for the analysis of volatiles and semi-volatiles started in 1992 when a Varian Model 8100 autosampler was adapted for the analysis of benzene, toluene, ethyl benzene, and xylene[4]. The idea of using multi-fiber SPME and desorption on a 96-well microplate format was initially introduced in 2005[31]. This idea was appealing for SPME-LC applications, as extraction and desorption are the most time-consuming steps due to slow mass transfer in the liquid phase. In SPME-LC, after extraction of analytes from the sample onto the fibers, the analytes can be desorbed from the fibers using liquid desorption, and then injected into a High-Performance Liquid Chromatography (HPLC) system. Each fiber is aligned to the corresponding well of a 96-well microplate. Agitation method including magnetic stirring, mechanical shaking, and sonication can be used to speed up the equilibrium between the SPME fibers and well contents in the microplate.

The design of parallel format and automation was achieved by introducing a commercially available automated sample preparation station called Concept 96 robotic system, made by PAS Technology (Magdala, Germany)[32,33]. The automated system consisted of a three-arm robotic autosampler that was fully controlled with software and two orbital agitators, as shown in Figure 1.4. This design has been applied to analyze drug compounds[33,34], polycyclic aromatic hydrocarbons (PAHs)[35], as well as fungal toxins[32] in biological fluids and other media [36].

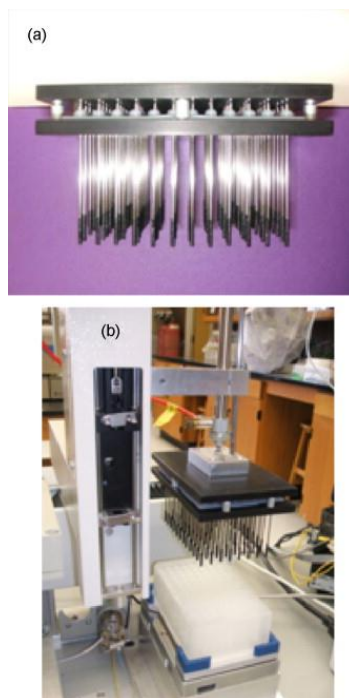


**Figure 1.4 (a) 96-well multi-fiber SPME device (stainless steel fibers coated with carbon tape). (b) robot arm inserting the multi-fiber SPME device in the 96-well plate. Reprinted with permission from reference[32]. Copyright (2008) Elsevier.**

## **1.2 METHODS FOR MEASUREMENT OF ACID DISSOCIATION CONSTANT**

The acid dissociation constant, expressed as the  $pK_a$  value, is a fundamental property of weak acids and bases. For compounds with a single ionized group, it is defined as the pH at which a compound is 50% ionized. Once the  $pK_a$  value is established, the extent of ionization at any pH for that compound is easily calculated. This is an important property for pharmaceutically active molecules since the physical, chemical, and biological properties of the neutral and ionized drugs are generally different. To measure  $pK_a$  values, it is necessary to put the sample in environments of various pH values and monitor a particular property that changes

as a function of the ionization state of the molecule. Traditional methods used to determine  $pK_a$  values usually rely on potentiometry or spectroscopy.

Historically, potentiometric titration is the standard method for the determination of  $pK_a$  values. In this method, the sample is titrated with an acid or base using a pH electrode to monitor the course of the titration. Spectrophotometric titrations are generally considered the main alternative to potentiometric titrations for  $pK_a$  measurements. The spectroscopic approach to  $pK_a$  measurement is commonly performed by NMR spectroscopy[37] or UV absorption[38]. The former technique analyzes chemical shift values as a function of pH in terms of a single titration curve to determine  $pK_a$ . The NMR method is relatively accurate and reliable but requires expensive and sophisticated instrumentation. The latter technique has high sensitivity for compounds with favorable molar absorptivity[39]. In this case, however, a chromophoric center must exist in the sample close to the ionizable groups so that the neutral and ionized forms show sufficiently different UV absorbances. Capillary electrophoresis (CE) has also been proposed as a technique for convenient and precise determination of aqueous  $pK_a$ [40,41]. This method relies on the principle that the solute shows an electrophoretic mobility relationship with pH values. In its uncharged state, the solute has no mobility, while in its completely ionized state, it has a maximum mobility. Acid dissociation constants can be determined by regression analysis of plot of mobility with pH values. This method offers several attractive features: it only requires small amounts of sample, is highly automated, and does not require precise information of sample concentration but only migration times.

In this dissertation, acid dissociation constant of ionizable compounds has been determined by a parallel polymer-based microextraction method. It measures acid dissociation constant while measuring intermolecular binding constants or other physicochemical properties

including lipophilicity as a function of pH. This parallel approach uses small amounts of sample and minimal amounts of organic solvent.

### 1.3 METHODS FOR LIPOPHILICITY MEASUREMENT

Lipophilicity is described by either partition coefficient (P) or distribution coefficient (D), which is a measure of how well a molecule partitions between a lipid and water. As discussed in Session 1.1.2, P and D are identical if only neutral species are considered. As suggested by Collander[42] and Leo[43],  $\log P_{ow}$ , the logarithmic value of the 1-octanol/water partition coefficient, has been widely recognized in the pharmaceutical, biomedical, and environmental fields to describe lipophilicity of various compounds. Many experimental methods exist to measure  $\log P_{ow}$  values.

Traditionally, the shake-flask procedure is a standard method to determine  $\log P_{ow}$  in the range of -2 to 4 [44]. In this method, the substance of interest is introduced into a separatory funnel with the two phases (1-octanol and water). The funnel is then shaken for a period long enough to reach equilibrium. The concentration of the test substance in each phase is determined after phase separation and  $\log P_{ow}$  is calculated. This method is time consuming, labor intensive, and requires relatively large amounts of pure compounds[45,46]. In addition, the octanol/water emulsions can be severe problems for compounds having a  $\log P_{ow}$  value larger than 4 [40,45].

The HPLC method is an indirect way to estimate  $\log P_{ow}$  values in the range of 0-6 and has also become a standard method[47]. A series of reference compounds are injected into a C<sub>18</sub> column. The retention factors of those compounds are used to create a calibration curve with their known  $\log P_{ow}$  values. Compounds with unknown  $\log P_{ow}$  values are then injected, and

their  $\log P_{ow}$  can be predicted by their retention time from the calibration curve[48]. This technique is rapid, precise and reproducible for sets of similar compounds, although impurities may make interpretation of the results difficult due to uncertainty in peak assignments. The reference compounds should be preferably similar to those being studied and difficulties arise if suitable standards are unavailable. One further disadvantage with this method is that HPLC is less suitable for molecules in ionic form since charged molecules have a far more complex retention behavior[45].

Recent advances in combinatorial technology have encouraged the development of lipophilicity measurement methods to be rapid, high throughput, and operational on the micro-scale. To increase the throughput of  $\log P_{ow}$  measurement, an attempt has been made to transfer the traditional shake-flask method to a 96-well format.[49] However, restrictions of the shake-flask method still remained due to octanol/water emulsions. Most of the current experimental methods only measure partition coefficients of the neutral species. Novel methods are needed with capability of measuring distribution coefficients and extension of applicable  $\log P_{ow}$  range.

## 1.4 OUTLINE

Lipophilicity and acid dissociation constants are important physicochemical properties that in part determine the suitability of an organic molecule as a pharmacological agent. Intermolecular associations are omnipresent in chemical and biochemical systems and particularly important in the efficacy of an excipient for a poorly soluble drug. Current standard methods to determine lipophilicity require large amounts of pure sample and have problems due to emulsion formation. This dissertation describes a method based on distribution of the solutes

between a polymer phase and an aqueous phase in a 96-well format, in the presence and absence of a receptor (e.g., candidate excipient) in one of the two phases. Figure 1.5 illustrates the general experimental design of this parallel approach. Briefly, polymer films are first prepared in 96-well microplates. Aqueous buffered solutions are then dispensed into the microplates. A solute or receptor can be embedded in either the polymer phase or the aqueous phase.

This parallel approach uses minimal amounts of organic solvent and only requires small amounts of sample. This approach has been used to determine polymer-water distribution coefficients of solutes. In addition, by measuring polymer-water distribution coefficients under a variety of experimental conditions, such as pH and receptor concentration, acid dissociation constants and solute-receptor binding constants have been successfully determined for several chemical systems.

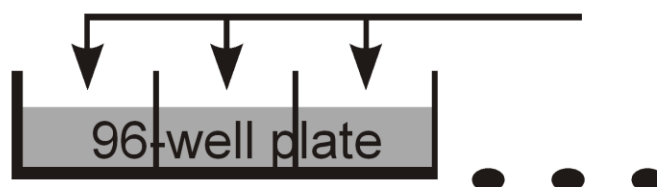
Chapter 2 of this dissertation focuses on using this parallel approach to determine drug-cyclodextrin binding constants. Drug and Cyclodextrin form inclusion complex in the aqueous solutions. Distribution coefficients of drugs between the polymer phase and the aqueous phase have been used to measure binding constants of drug-cyclodextrin inclusion complex. The polymeric phase was poly(vinyl chloride) (PVC) plasticized by 67% (w/w) dioctyl sebacate (DOS). Binding constants of a poorly water-soluble drug, econazole, with six cyclodextrins in aqueous solutions have been measured. The acid dissociation constant of econazole was also determined by measuring econazole-cyclodextrin binding constants at various pH values.

Chapter 3 describes the application of this parallel design to screen distribution coefficients of novel drug-like compounds. Distribution coefficients and acid dissociation constants of twenty-four novel drug-like compounds have been determined by this parallel approach and compared to the values calculated by commercially available software. The

software packages did not adequately predict experimental results, especially for ionizable compounds. This emphasizes the need for laboratory separations-based measurements of distribution coefficients. The polymeric phase was also PVC plasticized by 67% (w/w) DOS.

Finally, in chapter 4, intermolecular association has been studied in Teflon AF 2400, a fluorinated polymer phase, with and without fluorinated hydrogen bond donor Krytox 157 FSH in the 96-well approach. We found that the addition of a fluorinated carboxylic acid (Krytox 157 FSH) to a fluorinated film (Teflon AF 2400) increased the polymer-water distribution coefficients of quinoline, a nitrogen heterocycle. In addition, a novel fluorinated receptor-doped fiber solid phase microextraction (SPME) was developed to selectively detect quinoline in aqueous solutions. Compared to a commonly used SPME fiber made of polydimethylsiloxane (PDMS), it showed a preference for the nitrogen heterocyclic compound over a non-heterocyclic control, phenol. To our knowledge, this is the first reported receptor-doped fluorinated SPME.

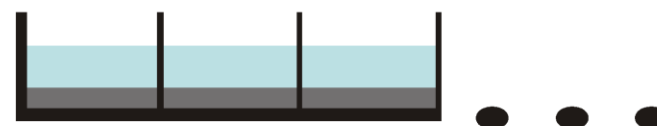
Add polymer/plasticizer solution  
with or without solute  
with or without receptor



Evaporate organic solvent



Add aqueous buffer solution  
with or without solute  
with or without receptor  
Equilibrate (const. T)



Transfer the aqueous phase  
Measure solute concentration  
by HPLC/plate reader

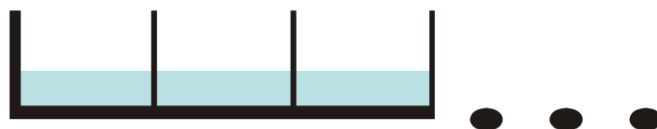


Figure 1.5 General procedure of the parallel experimental design to study intermolecular association and physicochemical properties

## **2.0 DETERMINATION OF DRUG-CYCLODEXTRIN BINDING CONSTANTS BY A HIGH-THROUGHPUT PHASE-DISTRIBUTION METHOD**

Part of this chapter has been published in *J. Pharm. Sci.*, 2009, 98, 229. Reproduced with permission from *J. Pharm. Sci.*. Copyright (2009) John Wiley & Sons.

### **2.1 INTRODUCTION**

Aqueous solubility is one of the fundamental determinants in developing new chemical entities as successful drugs.[50] According to recent estimates[51,52], nearly 40 % of new drugs are rejected because of poor biopharmaceutical properties. The main biopharmaceutical properties include solubility, stability,  $pK_a$ , bioavailability, brain penetration, and hepatotoxicity. Solubility, especially aqueous solubility is the most important one. Low aqueous solubility can limit drugs' function on human bodies. Compounds with an aqueous solubility of less than 100  $\mu\text{g/mL}$  may require development of a special formulation to overcome poor absorption properties.[53]

To solve this problem, pharmaceutical companies are giving strategies to measure, predict and improve solubility of promising new drug candidates during the preclinical phases of drug development. Multiple formulation techniques exist to increase the apparent solubility of lipophilic compounds without decreasing their optimized potency. These techniques include

particle size reduction, pH adjustment, addition of solubilizing excipients, solid dispersion, microemulsification, nanocrystallization, inclusion complex formation, etc[54].

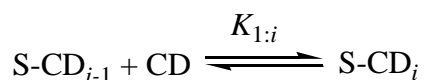
Cyclodextrins (CDs) are bucket-shaped oligosaccharides produced from starch, with a hydrophilic outer surface and a lipophilic inner cavity. They can form water-soluble inclusion complexes with many lipophilic compounds. They are commonly used in pharmaceutical formulations to enhance drug solubility, stability and bioavailability.[55,56] To date, there are more than 20 marketed drugs that contain CDs,[57] and numerous publications are emerging every year studying the use of CDs for drug formulation and delivery. Although higher order complexes are not uncommon, the simplest and most frequent stoichiometry of drug-cyclodextrin (S-CD) complexes is 1:1



The binding constant ( $K_{1:1}$ ) is defined as

$$K_{1:1} = \frac{[S-CD]}{[S][CD]} \quad \text{Equation 2.1}$$

where [S], [CD], [S-CD] are the concentrations of the free drug, free CD, and drug-CD complex, respectively. For consecutive complexation



The binding constant ( $K_{1:i}$ ) is defined as

$$K_{1:i} = \frac{[S-CD_i]}{[S-CD_{i-1}][CD]} \quad \text{Equation 2.2}$$

The binding forces within the drug-CD complexes may involve hydrophobic, van der Waals, hydrogen bonding, or dipole interactions.[58] Depending on the cavity size and functional groups, CDs vary in their ability to form inclusion complexes with specific guest

compounds.[59] The stoichiometry and binding constant are important in any investigation to assess the value of a CD for the formulation of a specific drug.[60]

Various techniques exist to measure drug-CD binding constants. The most common method to determine  $K_{1:1}$  for drug-CD binding is the Higuchi-Connors phase-solubility method.[61] This method measures the effect of CD concentration on the apparent solubility of the drug. The intrinsic solubility ( $S_0$ ) and the slope of the solubility versus CD-content diagram are then used to calculate  $K_{1:1}$ . There are also a few reports using phase-distribution methods to determine binding constants for CD complexes.[62,63]

Recently, we have developed a high-throughput method that can determine the distribution behavior of drug candidates between a polymer phase and an aqueous phase.[27] This method has also been applied to measure intermolecular associations in the polymer phase to screen chiral selectors.[64] In this chapter of work, we report the application of this high-throughput method for the determination of drug-CD binding constants in the aqueous phase. The polymer phase is composed of poly (vinyl chloride) (PVC) and dioctyl sebacate (DOS) at the ratio of 1:2 (w/w). Econazole (Figure 2.1) is an anti-fungal drug, which has very low aqueous solubility of 5  $\mu\text{g/mL}$  at 25  $^{\circ}\text{C}$ . Its ability to form water-soluble complexes with various CDs was determined.

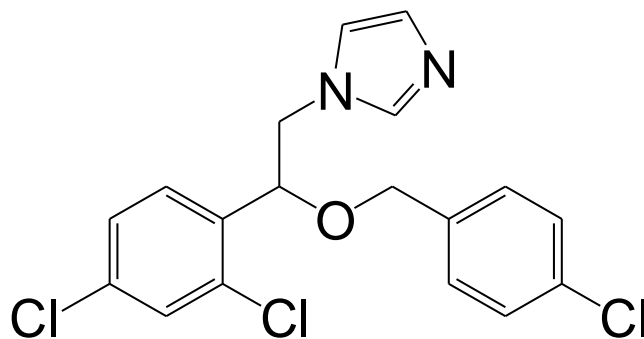


**Figure 2.1 Structure of econazole**

## 2.2 EXPERIMENTAL

### 2.2.1 Materials

(2-hydroxyethyl)- $\beta$ -cyclodextrin (HE- $\beta$ -CD), (2-hydroxypropyl)- $\beta$ -cyclodextrin(HP- $\beta$ -CD), 2,6-di-O-methyl- $\beta$ -cyclodextrin(DM- $\beta$ -CD), heptakis (2,3,6-tri-O-methyl)- $\beta$ -cyclodextrin (TM- $\beta$ -CD),  $\alpha$ -cyclodextrin( $\alpha$ -CD),  $\beta$ -cyclodextrin( $\beta$ -CD) were purchased from Sigma-Aldrich-Fluka with the highest available purities. Econazole free base was purchased from Molecula Ltd. (Dorset, UK). HPLC grade tetrahydrofuran (THF) and acetonitrile (ACN) were purchased from Aldrich (Milwaukee, WI). PVC (high molecular weight) and dioctyl sebacate (DOS) were purchased from Fluka (Ronkonkoma, NY). Water used in all the experiments was purified with a Milli-Q Synthesis A10 system (Millipore, Bedford, MA). Costar polypropylene 96-well microplates (flat-bottom, 330- $\mu$ L well volume) and thermal adhesive sealing films were purchased from Fisher Scientific Co. (Pittsburgh, PA).

### 2.2.2 Equipment

An UltraSpense 2000 microplate dispenser (KD Scientific, Holliston, MA) was used to prepare polymer films in 96-well plates. A Zipvap-96 well evaporator (Chrom Tech, Apple Valley, MN) was used to evaporate THF. A Deep Well Maximizer (or BioShaker) (Model M BR-022 UP, made by Taitec and distributed by Bionexus, Inc., Oakland, CA) was used to speed up the drug distribution kinetics and control the temperature for better reproducibility. An X-LC (Jasco, Inc.) UHPLC system was used to determine the econazole concentration with a UHPLC C<sub>18</sub> column (1.0  $\times$  50 mm, particle size: 1.7  $\mu$ M, Waters, Milford, MA).

### 2.2.3 Buffer Preparation

The phosphate buffer solutions (20 mM, pH 5.80, 6.62, 6.83, 7.12, 7.43, 8.46) were made by mixing appropriate amounts of 20 mM sodium phosphate dibasic solution and 20 mM sodium phosphate monobasic solution.

### 2.2.4 Preparation of Plasticized PVC Films

PVC (4.17 g) and DOS (8.33 g) were dissolved in 500 mL of THF in a volumetric flask. The microplate dispenser was used to dispense the solution to the wells of a polypropylene 96-well microplate. The plate was placed in an evaporator for 15 min for evaporation of the THF, and the films were formed at the bottom of each well. The volume of each film was estimated as

$$V_{film} = \frac{12.5g / 500mL \times V_{solution}}{d_{film}} \approx \frac{V_{solution}}{100\mu L} \times 2.5\mu L \quad \text{Equation 2.3}$$

Here  $V_{solution}$  is the volume of the THF solution used in each well, and  $d_{film}$  is the density of the film which is estimated as 1 g/mL. In our experiments in this part of work, 100  $\mu$ L of the THF solution was dispensed in each well, so the volume of each film was  $\sim$ 2.5  $\mu$ L.

### 2.2.5 High-Throughput Phase-Distribution Studies

Figure 2.2 gives the sequence of operations for the phase-distribution method that measures the binding constants of drug-CD complexes. The plasticized PVC films were prepared in polypropylene 96-well microplates. Briefly, an appropriate amount of the DOS-plasticized PVC THF solution and the drug THF solution are mixed at a ratio of 1:1. Aliquots of 200  $\mu$ L of

this solution were dispensed by the microplate dispenser to microplates. Evaporation of solvent allowed the formation of polymer films at the bottom of each well. The volume of each film has been calculated to be  $\sim 2.5 \mu\text{L}$  according to Equation 2.3. CD-containing aqueous buffers ( $200 \mu\text{L}$ ) were then manually dispensed over the films. The plates were covered by adhesive sealing films and incubated in a shaker ( $500 \text{ rpm}$ ,  $25 \text{ }^\circ\text{C}$ ). In order to determine the equilibration time, the concentration of drug extracted into the aqueous phase was measured as a function of time at pH 7.4. Other than for this experiment, all data generated were at equilibrium. To determine the drug concentration, the supernatant from each well was transferred to another plate and injected to the HPLC system by an autosampler. The distribution ratio of concentrations in the aqueous phase over the polymer phase, was then calculated as

$$D_{wp} = \frac{C_E}{(C_S - C_E) \cdot \Phi} \quad \text{Equation 2.4}$$

Here  $C_S$  is the drug aqueous concentration if all the target has been extracted to the aqueous phase,  $C_E$  is the drug aqueous concentration at equilibrium, and  $\Phi$  is the phase ratio (aqueous over polymer).

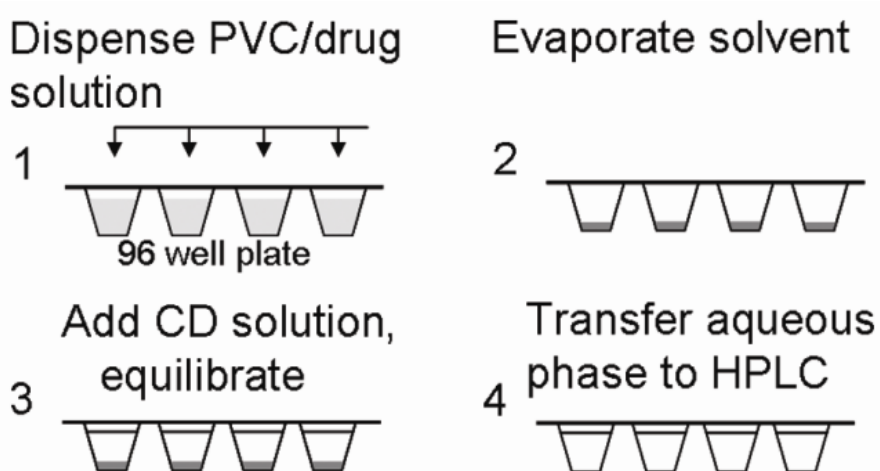


Figure 2.2 Schematic illustration of the preparation and use of polymer films in 96-well plates

## 2.2.6 HPLC Method to Determine Econazole Concentration

The column used was the Waters UPLC C<sub>18</sub> column. The mobile phase was acetonitrile/H<sub>2</sub>O (65/35, v/v), with a flow rate of 0.2 mL/min. The back-pressure was ~7000 psi. To ensure reproducibility, the full-load injection mode was used (injection volume 10 μL; loop volume 5 μL). Detection was by UV absorbance at 210 nm. The peak area was used for the calibration and determination of sample concentration. The time per analysis is ~60 s.

## 2.2.7 DOS binding to CDs.

A 2.5 mL solution of 10 % ( w/v) HP-β-CD was equilibrated with pure DOS for one day at 25 °C. HPLC of the aqueous phase (UPLC C18 column, mobile phase 90% acetonitrile, 10% water, flowing at 0.13 mL/min) showed no obvious DOS peaks. A standard of DOS had a retention time of 1.7 minutes. Detection was at 210 nm (absorbance).

## 2.3 RESULTS AND DISCUSSION

### 2.3.1 Theories to Determine the Stoichiometry n and Binding Constants K<sub>1:i</sub> (i = 1 to n)

The distribution of the free drug between the aqueous phase and the film phase is determined by the distribution coefficient  $D_0$ :

$$D_0 = \frac{[S]}{[S]_{film}}$$

Equation 2.5

where  $[S]$  and  $[S]_{film}$  are the free drug concentration in the aqueous phase and film phase, respectively. When the CD is added to the aqueous phase, the drug distribution coefficient is:

$$D = \frac{[S] + \sum_{i=1}^n [S \cdot CD_i]}{[S]_{film}} \quad \text{Equation 2.6}$$

where  $n$  is the stoichiometry,  $[S \cdot CD_i]$  ( $i = 1$  to  $n$ ) is the drug-CD complex concentration in the aqueous phase in various forms. Dividing Equation (2.6) by Equation (2.5):

$$\frac{D}{D_0} = 1 + \sum_{i=1}^n \frac{[S \cdot CD_i]}{[S]} \quad \text{Equation 2.7}$$

From Equation (2.2), one obtains:

$$[S \cdot CD_i] = [S][CD]^i \prod_{j=1}^i K_{1,j} \quad \text{Equation 2.8}$$

Inserting Equation (2.8) to Equation (2.7):

$$\frac{D}{D_0} = 1 + \sum_{i=1}^n \left( [CD]^i \prod_{j=1}^i K_{1,j} \right) \quad \text{Equation 2.9}$$

It is known that  $pK_a$  of econazole is 6.69.[48] If system is acidic, the cationic form of econazole should also be considered in the equation as follows. The distribution of the free neutral and cationic drug between the aqueous phase and the film phase is determined by the distribution coefficient  $D_0$ ,

$$D_0 = \frac{[S] + [HS^+]}{[S]_{film} + [HS^+]_{film}} \quad \text{Equation 2.10}$$

where  $[HS^+]$  and  $[HS^+]_{film}$  are the free neutral and cationic drug concentration in the aqueous phase and film phase, respectively. When the CD is added to the aqueous phase, the drug distribution coefficient is:

$$D = \frac{[S] + \sum_{i=1}^n [S \cdot CD_i] + [HS^+] + \sum_{i=1}^n [HS^+ \cdot CD_i]}{[S]_{film} + [HS^+]_{film}} \quad \text{Equation 2.11}$$

Dividing Equation (2.11) by Equation (2.10):

$$\frac{D}{D_0} = 1 + \sum_{i=1}^n \frac{[S \cdot CD_i] + [HS^+ \cdot CD_i]}{[S] + [HS^+]} \quad \text{Equation 2.12}$$

It is known that the equation for the acid dissociation constant  $K_a$  is

$$K_a = \frac{[S][H^+]}{[HS^+]} \quad \text{Equation 2.13}$$

Inserting Equation (2.8) and Equation (2.13) into Equation (2.12):

$$\frac{D}{D_0} = 1 + \sum_{i=1}^n \frac{[CD]^i \left( \prod_{j=1}^i K_{1;j} + \frac{[H^+]}{K_a} \prod_{j=1}^i K_{1;j}^+ \right)}{1 + \frac{[H^+]}{K_a}} \quad \text{Equation 2.14}$$

where  $K_{1;j}^+$  is the binding constant of cationic drug and cyclodextrin.

If the system is very acidic,

$$\frac{[H^+]}{K_a} \gg K_{1;j} > 1$$

Equation (2.14) will become

$$\frac{D}{D_0} = 1 + \sum_{i=1}^n \left( [CD]^i \prod_{j=1}^i K_{1;j}^+ \right) \quad \text{Equation 2.15}$$

If the cationic form of the drug is ignored, Equation (2.14) will become Equation (2.9) again.

Plotting  $D/D_0$  versus  $[CD]$ , the stoichiometry and the binding constants can be obtained from polynomial fitting analyses. In practice, a degree one (linear) fitting should first be performed, assuming that only 1:1 complex forms

$$\frac{D}{D_0} = 1 + K_{1:1}[CD] \quad \text{Equation 2.16}$$

A proper fitting should give a straight line with a y-intercept of unity, and the slope can report the value of  $K_{1:1}$ . Otherwise linear regression on a quadratic equation should be carried out, assuming that both 1:1 and 1:2 complexes form:

$$\frac{D}{D_0} = 1 + K_{1:1}[CD] + K_{1:1}K_{1:2}[CD]^2 \quad \text{Equation 2.17}$$

Again, a correct fitting should give a y-intercept of unity, and the  $K_{1:1}$  and  $K_{1:2}$  values can be obtained from the corresponding coefficients of the polynomial. If the fit is still not satisfactory, fitting analyses with higher degrees should be continued. Note that all the coefficients of the polynomial should have positive values. In this study, the concentration of CD prepared in the aqueous buffer ( $C_{CD}$ ) is much higher than the drug concentration ( $C_S$ ), hence the drug-CD complexation does not significantly change the free CD concentration, and  $[CD]$  in those equations can be reasonably replaced by  $C_{CD}$ .

### 2.3.2 Experimental Results and Discussion

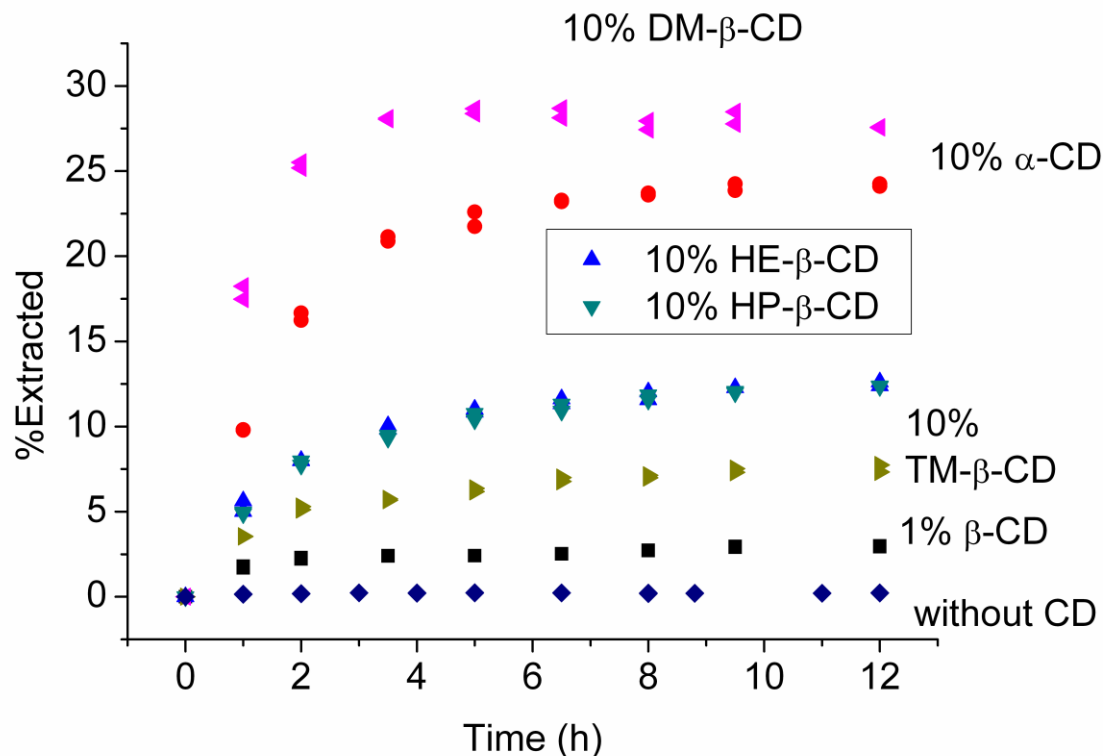


Figure 2.3 Percentage of econazole extracted as a function of time in the presence of six CDs and without CD

A kinetic study was first performed to determine the time needed for the phase distribution of econazole to reach equilibrium. The results are shown in Figure 2.3. Clearly, 8-9.5 h is enough for all the distribution experiments to be equilibrated. Careful inspection of the curves shows that the equilibration time is shorter when the aqueous phase contains less CD or the specific CD has a weaker ability to extract econazole. It also shows that the equilibration time for econazole in the absence of CD in the aqueous phase is about 4 h. Also, very low percentage of econazole has been extracted into the aqueous phase without CD, which is

consistent with the fact econazole has very low aqueous solubility ( $5 \mu\text{g/mL}$  at  $25^\circ\text{C}$ ). Based on the kinetic data, all other distribution experiments were allowed to equilibrate for 10 h.

Instructed by Equation (2.9), the effect of CD concentration on the distribution of econazole was then studied. Figure 2.4 gives the profile of econazole equilibrium concentration versus CD-content in the aqueous phase for six CDs. Each measurement was repeated for four times and the corresponding error bar indicates the standard error of the mean (SEM). The SEM values were then used in error propagations to determine the errors of the calculated distribution ratios and  $D/D_0$  values. Apparently, at higher CD concentration, more econazole is extracted to the aqueous phase. For these six CDs, the ability to extract econazole is in the order of DM- $\beta$ -CD >  $\alpha$ -CD >  $\beta$ -CD > HE- $\beta$ -CD  $\approx$  HP- $\beta$ -CD > TM- $\beta$ -CD, which is in good agreement with the previous kinetic study (Figure 2.3) and reported phase-solubility data of several CDs ( $\alpha$ -CD >  $\beta$ -CD > HP- $\beta$ -CD).[65] Various structures of CDs explain their different binding abilities with econazole. Linear regression on Equation (2.17) gives the  $K_{1:1}$  and  $K_{1:2}$  values, as shown in Table 2.1. The errors are their standard deviations. Some of the fitted curves are shown in Figure 2.5 and all the coefficients of determination (COD) are listed in Table 2.1. The econazole-CD binding constants ( $K_{1:1}/10^3 \text{ M}^{-1}$ ) discovered by phase-solubility studies have been reported for  $\alpha$ -CD, HP- $\beta$ -CD, and  $\beta$ -CD, which are  $2.63 \pm 0.26$ ,  $1.54 \pm 0.15$ , and  $1.42 \pm 0.13$ , respectively.[65] These values are in the same order of magnitude as the data in Table 2.1, however, because the conditions of the experiments differ, the results do not agree quantitatively. Since the pH and choice of buffer species have a great effect on the determination of binding constant,[65] the literature values measured in pure water should only be used for qualitative purposes. The  $K_{1:2}$  values are larger than zero, indicating the formation of 1:2 complexes. All  $K_{1:2}$  values are highly significant as judged by p values. Probabilities that the values of  $K_{1:2}$  are different from zero

based only on chance all  $< 0.0001$  except for the final entry in Table 2.1 ( $\beta$ -CD) in which case it is  $< 0.001$ . Most studies on imidazole-CD complexation have assumed a 1:1 ratio,[50,66] but higher order complexes have also been reported.[67-71] For instance, the stoichiometry of econazole/ $\beta$ -CD has been published by several groups to be 1:1,[65,72] while a study has discovered the formation of 2:3 complex.[67]

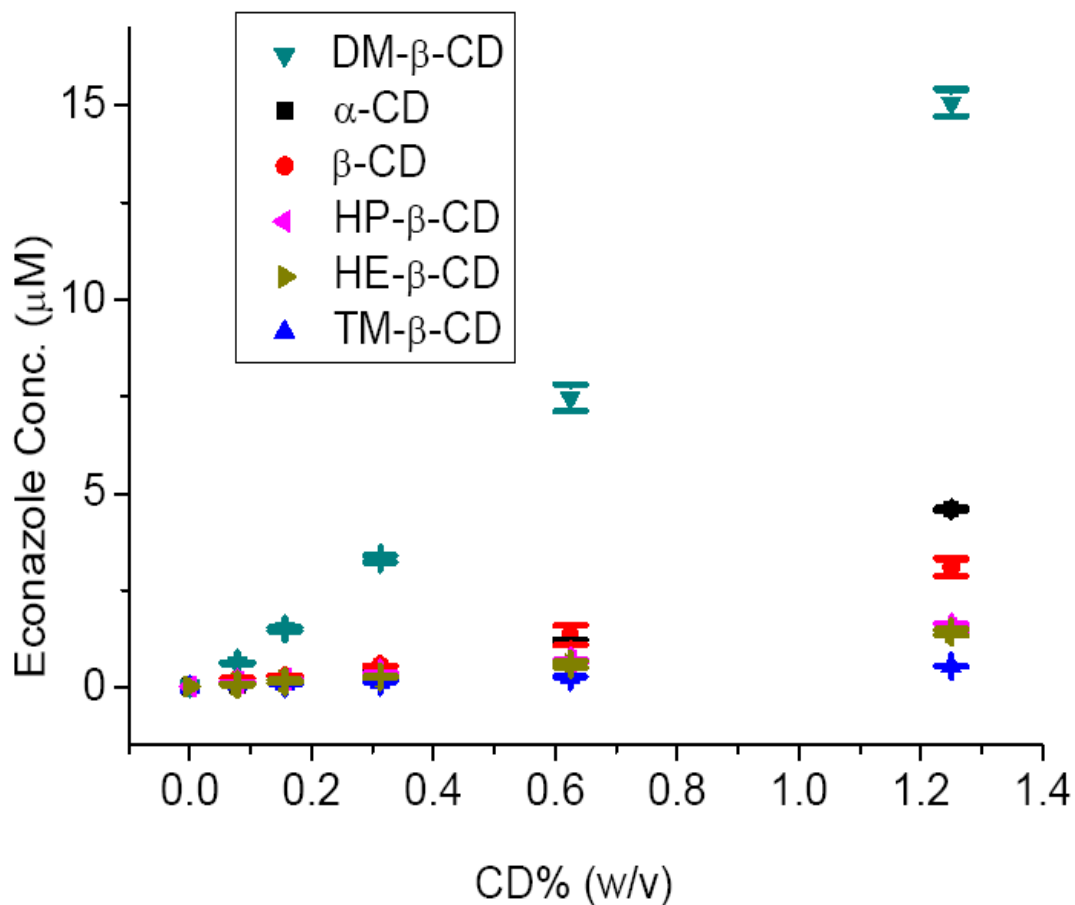
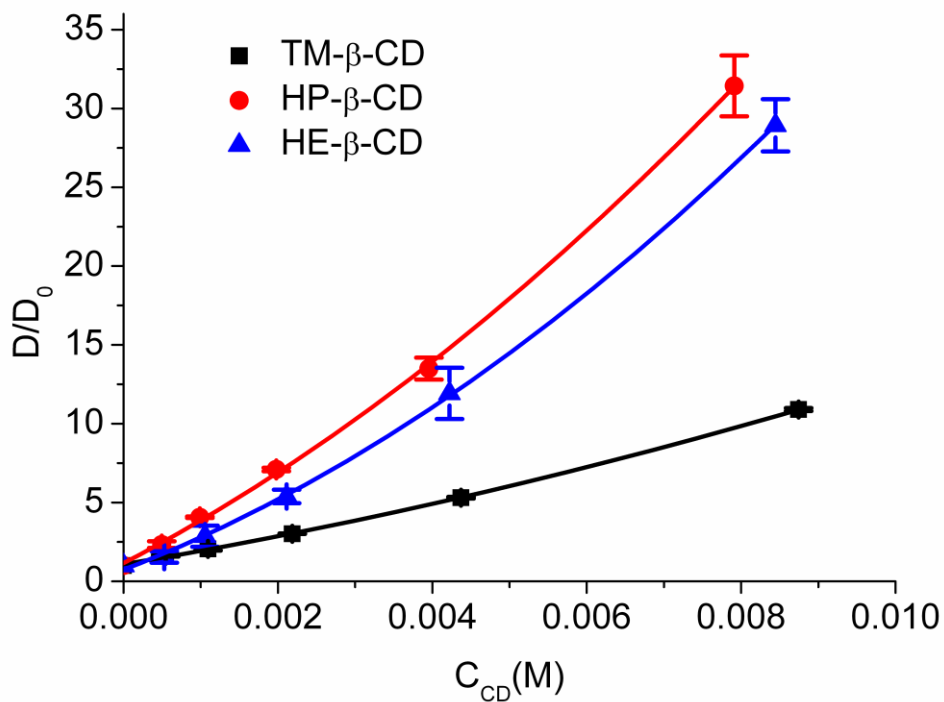


Figure 2.4 Effect of CD concentrations on econazole equilibrium concentration in the aqueous phase

**Table 2.1 Binding constants of econazole with six CDs**

| $D_0$                            | Cyclodextrin    | M.W. (g/mol)  | $K_{1:1}$ ( $10^3 \text{ M}^{-1}$ ) | $K_{1:2}$ ( $\text{M}^{-1}$ ) | COD    |
|----------------------------------|-----------------|---------------|-------------------------------------|-------------------------------|--------|
| $(1.20 \pm 0.09) \times 10^{-5}$ | HE- $\beta$ -CD | $\sim 1480^a$ | $3.98 \pm 0.13$                     | $4.9 \pm 0.5$                 | 0.9989 |
|                                  | HP- $\beta$ -CD | $\sim 1580^a$ | $3.90 \pm 0.22$                     | $10.0 \pm 1.9$                | 0.9976 |
|                                  | DM- $\beta$ -CD | $\sim 1330^a$ | $29.3 \pm 2.2$                      | $57.7 \pm 8.7$                | 0.9982 |
|                                  | TM- $\beta$ -CD | 1429.54       | $0.66 \pm 0.04$                     | $53.9 \pm 3.7$                | 0.9994 |
|                                  | $\alpha$ -CD    | 972.84        | $1.78 \pm 0.30$                     | $256 \pm 44$                  | 0.9997 |
|                                  | $\beta$ -CD     | 1134.98       | $4.08 \pm 0.50$                     | $47.6 \pm 12.1$               | 0.9956 |

<sup>a</sup> Randomly substituted. Their average molecular weights are determined by ESI-MS.



**Figure 2.5 Multivariate linear regression results for fitting  $D/D_0$  versus CD concentration.**

**Table 2.2 Binding constants of econazole with HP- $\beta$ -CD at various temperatures**

| Temperature (K) | $K_{1:1}$ ( $10^3 \text{ M}^{-1}$ ) | COD    |
|-----------------|-------------------------------------|--------|
| 293.15          | $2.06 \pm 0.009$                    | 0.9999 |
| 298.15          | $1.81 \pm 0.005$                    | 0.9999 |
| 303.15          | $1.50 \pm 0.016$                    | 0.9992 |
| 308.15          | $1.34 \pm 0.008$                    | 0.9999 |

The binding behavior of econazole to HP- $\beta$ -CD has been studied at various temperatures. The  $K$  values were measured at 293, 298, 303, and 308 K, respectively, which are shown in Table 2.2. Since the binding constant is related to the Gibbs free energy ( $\Delta G^0$ ) of complexation, which comes from enthalpic ( $\Delta H^0$ ) and entropic ( $\Delta S^0$ ) terms, these thermodynamic terms can provide insight into the driving forces for complexation. The thermodynamic parameters for inclusion processes were determined from the temperature dependence of the binding constants using a *van's Hoff* plot ( $\ln K$  versus  $1/T$ ), as seen in Figure 2.6. The plot was linear with a correlation coefficient close to unity ( $R^2 \geq 0.99$ ) within the temperature range considered in the present study, indicating that the changes in the heat capacity could be neglected.

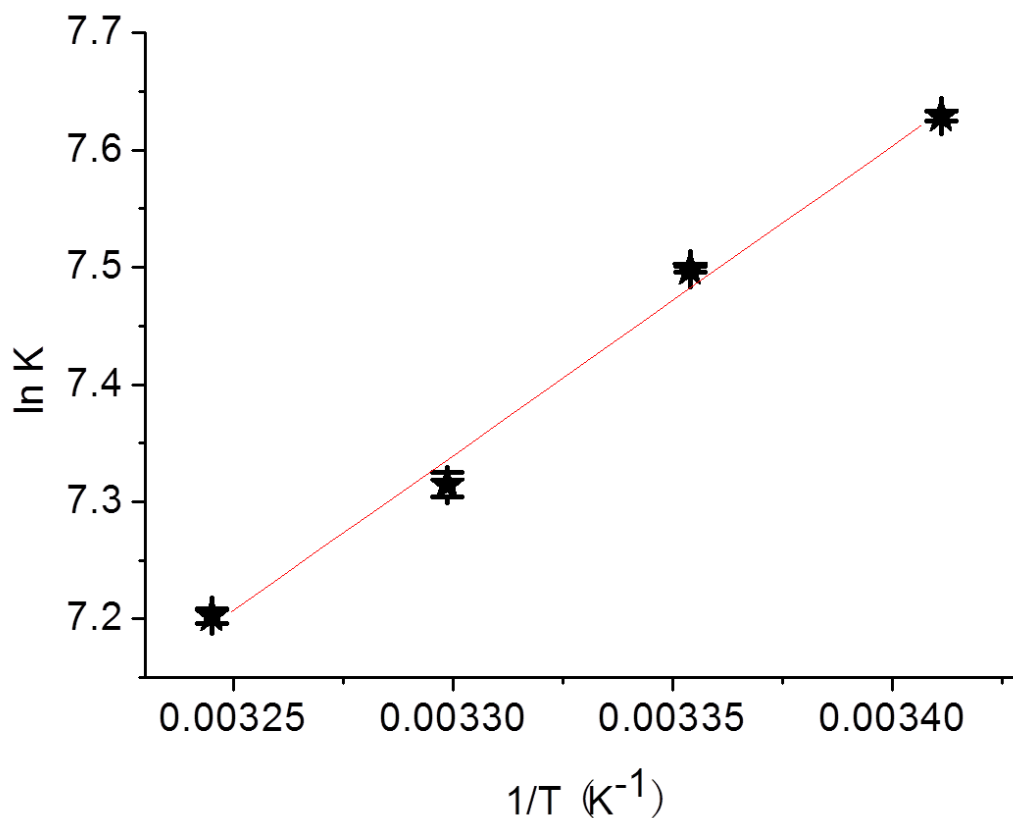


**Figure 2.6** van't Hoff plot for econazole - HP-β-CD complex

The standard Gibbs free energy change of the binding was calculated using the following relations:

$$\Delta G^0 = -RT \ln K = \Delta H^0 - T\Delta S^0 \quad \text{Equation 2.18}$$

where the  $\Delta H^0$  and  $\Delta S^0$  can be deduced from the slope and the intercept of the *van's Hoff* plot, respectively. In our experiment,  $\Delta H^0$  was  $-22.0 \pm 1.4$  kJ/mol,  $\Delta S^0$  was  $-11.5 \pm 4.5$  J/ (mol\*K),  $\Delta G^0$  (298K) was  $-18.6 \pm 1.9$  kJ/mol. The following conclusions can be made from the data:

(1) The  $K$  values decrease with rising in temperature, *i.e.*, as the temperature increases, the affinity of the cyclodextrin for the drug decreases. This phenomenon is because the formation of the complex is exothermic ( $\Delta H^0 < 0$ ).

(2) The negative value of  $\Delta G^0$  suggests that the complexation is thermodynamically favored. The drug binds to CD with a favorable enthalpic term ( $\Delta H^0$  is less than zero) and an unfavorable entropic term ( $\Delta S^0$  is less than zero). Also, the complex formation is enthalpy driven ( $|\Delta H^0| > T|\Delta S^0|$ ).

(3) The effect of temperature on drug-CD binding has also been studied by Shehatta *et al.*[73] Their obtained the binding constant of itraconazole with HP- $\beta$ -CD was  $(1.17 \pm 0.101) \times 10^3 \text{ M}^{-1}$  in 298 K, which was lower than our measurement for econazole- HP- $\beta$ -CD complex ( $(1.81 \pm 0.005) \times 10^3 \text{ M}^{-1}$ ), also led to higher standard Gibbs free energy  $\Delta G^0$  (298K) value ( $-17.5 \pm 0.2 \text{ KJ/mol}$ ) than ours ( $-22.0 \pm 1.4 \text{ KJ/mol}$ ). Itraconazole has a larger size than econazole, which contributes to a less favorable affinity of the drug for CD, although their structures are similar. Different shapes and sizes results in the difference in the entropic term  $\Delta S^0$  ( $-40.0 \pm 4.7$  *versus*  $-11.5 \pm 4.5 \text{ J/(mol}\cdot\text{K)}$ ).

The influence of pH on the apparent binding constant of the econazole-HP- $\beta$ -CD inclusion complex has been studied. As shown in Figure 2.7, a decrease in pH results in a drop in the apparent binding constant ( $K = 2.15 \times 10^3 \text{ M}^{-1}$  at pH 8.5; whereas  $K = 0.654 \times 10^3 \text{ M}^{-1}$  at pH 5.8) indicating that binding constant is larger in the less protonated form for the econazole-HP- $\beta$ -CD complex. Thus, the inclusion process with neutral econazole is more favorable than with protonated econazole, which is consistent with literature observations[72]. More quantitatively and specifically, we have found that Equation (2.14) can be transformed to

$$\frac{D}{D_0} = 1 + \frac{K_{1:1} + K_{1:1}^+ * \frac{[H^+]}{K_a}}{1 + \frac{[H^+]}{K_a}} * [CD] = 1 + K_{1:1}^{App} * [CD] \quad \text{Equation 2.19}$$

Thus,

$$K_{1:1}^{App} = \frac{K_{1:1} + K_{1:1}^+ * \frac{[H^+]}{K_a}}{1 + \frac{[H^+]}{K_a}} = K_{1:1}^+ + \frac{K_{1:1} - K_{1:1}^+}{1 + 10^{pK_a - pH}} \quad \text{Equation 2.20}$$

where  $K_{1:1}$  is the binding constant of CD with neutral econazole,  $K_{1:1}^+$  is that with protonated econazole,  $K_{1:1}^{App}$  is the apparent binding constant of the complex, including CD with both neutral and protonated form. After applying nonlinear least-squares curve fitting, as shown in Figure 2.7, the  $K_{1:1}$ ,  $K_{1:1}^+$ , and  $pK_a$  values of econazole can all be obtained, which are  $(2.21 \pm 0.06) \times 10^3 \text{ M}^{-1}$ ,  $(0.47 \pm 0.09) \times 10^3 \text{ M}^{-1}$ , and  $6.75 \pm 0.08$ , respectively. The binding constant of CD with protonated econazole is smaller than that with neutral form, which confirms our previous qualitative conclusion that the inclusion complex between econazole and CD is hydrophobically driven. The measured  $pK_a$  ( $6.75 \pm 0.08$ ) is statistically indistinguishable from the literature value (6.69).

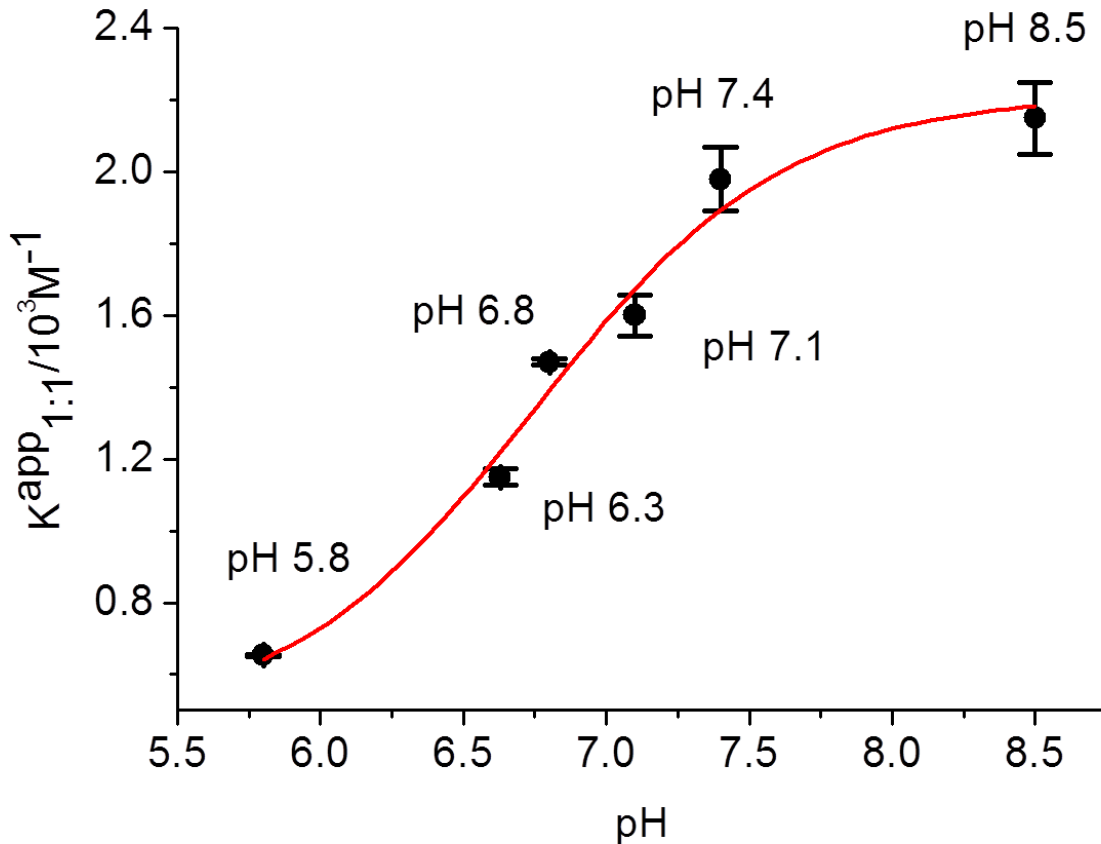


**Figure 2.7 Effect of pH on the apparent binding constant of the econazole-HP- $\beta$ -CD complex**

Compared to the phase-solubility method, which can require days for the dissolving of the drug to be saturated, this new technique is faster. Moreover, the drug amounts used in solubility experiments are much greater than in this method. For instance, the highest econazole concentration in a phase-solubility study is ~30 mM,[65] but in the phase-distribution experiment,  $C_S$  is less than 0.1 mM. In addition, the volume of the CD solution used in a solubility study is typically 10 mL, which is 40 times more than in this distribution experiment. These two factors have led to a 12000 fold decrease in material requirements. The equilibration time is shorter in these phase-distribution studies probably because it does not involve the

equilibrium between solid and dissolved drug. For other phase-distribution methods, which study the drug distribution between an organic solvent and an aqueous phase, the solvent-CD complexation may lead to misinterpretation. In addition, entrainment and emulsion can be severe problems for very hydrophobic compounds,[40] and the handling of small volumes of organic solvent may be difficult.[27]

In phase-solubility studies, several factors influence the accuracy of the final result. One such factor is the accurate and precise determination of the intrinsic solubility ( $S_0$ ). Similarly for this approach, the variance of  $D_0$  may lead to misinterpretation of  $n$  and  $K_{1:i}$  as well. Since the drug concentration is usually low ( $\sim 0.01$ - $0.1 \mu\text{M}$ ) when determining  $D_0$ , some error is inevitable. Ways to decrease the measurement error of  $D_0$  have been discussed elsewhere.[27] The most important aspect in getting an accurate value for  $D_0$  is the sensitivity and selectivity of the analytical method used to measure the concentrations of the solute. As far as precision is concerned, the 96-well plate approach is beneficial, as it is easy to do repeat measurements. Other potential errors may arise from the distribution process itself. The drug may adsorb to the plate surface. We have determined that this does not occur for a series of compounds ranging in their octanol-water partition coefficients over a logarithmic range of 0.5 to 3.2[48]. Another potential source of error is that DOS may associate with CDs, and thus compete with the drug and lead to inaccurate binding constants. In the experiments described herein, the CDs are in great excess over the drug, so competition is minimized. Nonetheless, we have determined that there is no detectable DOS extracted into aqueous solution containing 10 % (w/v) HP-  $\beta$  -CD.

All of the experiments except the kinetic study were carried out at equilibrium. It is worth noting that, in our experience, solute drug distribution at early times before equilibrium is correlated with the equilibrium concentration. As Figure 2.3 shows, after only one hour of

equilibration it is already obvious that 10% DM- $\beta$ -CD is best solubilizing agent for econazole. Although we have not investigated this thoroughly, it seems clear that screening to determine the rank order of the effectiveness of a series of potential solubilizers could be carried out much more rapidly than the equilibrium studies that we have discussed herein.

## 2.4 CONCLUSIONS

We have successfully developed a new method to measure the binding constants of drug-CD complexes in the aqueous phase using high-throughput technologies. This method measures the distribution behavior of a drug between a polymer phase and an aqueous phase in 96-well microplates. With four repeats, distribution ratios of econazole with respect to six CD-containing buffers at four different concentrations can be determined simultaneously. Multivariate linear regression has been established to give the binding constants of econazole to the six CDs respectively. Both 1:1 and 1:2 complexes are found and the calculated  $K_{1:1}$  can be correlated to some literature data from phase-solubility studies. The thermodynamic parameters of the complexation process have been calculated, indicating that the complex formation is exothermic and enthalpy driven ( $|\Delta H^0| > T|\Delta S^0|$ ). The binding constants of econazole to HP- $\beta$ -CD have been also studied at various pH conditions. An acidic environment weakens the binding between econazole with HP- $\beta$ -CD due to more favorable inclusion process with neutral econazole than with protonated form. Nonlinear fitting of the apparent binding constants with pH leads to binding constants of both the neutral and protonated form and  $pK_a$  of econazole. Compared to the phase-solubility method, our protocol is much faster. Moreover, the material requirement decreases four orders of magnitude. This method has great flexibility as well, for instance,

'multiplex' approaches are possible due to the much lower concentration of the drug relevant to the CD concentration. In addition, this method is possible to be fully automated.

### 3.0 LIPOPHILICITY SCREENING OF NOVEL DRUG-LIKE COMPOUNDS AND COMPARISON TO CLOGP

This chapter has been published in *J. Chromatogr. A*, 2012, 1258, 161. Reproduced with permission from *J. Chromatogr. A*. Copyright (2012) Elsevier.

#### 3.1 INTRODUCTION

Acid dissociation constants ( $pK_a$ s) and the logarithmic value of the 1-octanol/water partition coefficient ( $\log P_{ow}$ ) are important parameters in environmental, medical, toxicological and pharmaceutical studies of novel organic molecules. Sixty-three percent of the molecules listed in the 1999 *World Drug Index* are ionizable between pH 2 and pH 12[38]. Various ionized forms of a compound may differ in physical, chemical, and biological properties, so it is important to predict which ionic form of the molecule is present at the site of action. The partition coefficient is often used in combination with the  $pK_a$  value to predict the distribution of a compound in a biological or ecological system. This knowledge can be valuable in the estimation of drug absorption, distribution, metabolism, and excretion (ADME), or for the estimation of the distribution of a solute in an ecological system.

Numerous methods exist to measure or estimate the  $pK_a$  and  $\log P_{ow}$  values. The shake-flask method and RP-HPLC method are the main experimental methods to determine partition

coefficients. The shake-flask procedure is a standard method to determine octanol/water partition coefficients in the range of -2 to 4[46,74]. This method is the most reliable and accurate one, however, it is tedious, time consuming, and requires large amounts of pure material. In addition, octanol/water emulsions can be severe problems, especially for hydrophobic compounds, limiting the upper measurable  $\log P_{ow}$  value to 4[40]. Recently, a micro-volume flow extraction system consuming less than 1 mL of octanol and aqueous sample has been developed[75]. To increase sample throughput, the traditional shake-flask method has been automated and scaled down using 96-well plate technology and a robotic liquid handler[76]. However, the emulsion problem still exists for scaled down shake flask method, especially for hydrophobic compounds.

The RPLC method is an indirect but popular way to measure  $\log P_{ow}$  values in the range of 0-6[77]. This method is rapid and reproducible for sets of similar compounds, although impurities may make the interpretation of the results difficult due to uncertainty in peak assignments. However, it is not applicable to strong acids and bases, metal complexes, substances that react with the eluent, or surface-active agents[40]. One further disadvantage with this method is that the reference compounds should be preferably similar to those being studied and difficulties arise if suitable standards are unavailable.

There are some theoretical approaches to predict lipophilicity. Most of them add up the  $\log P_{ow}$  contribution from each fragment and then apply structure-based correction factors[46]. There are at least 20 software packages available at present, which provide convenient and fast prediction of lipophilicity for novel compounds. However, studies show calculations are not reliable for  $\log P_{ow}$  and  $pK_a$  of zwitterionic, tautomeric and charged compounds as well as for strong hydrogen-bonding compounds[78]. It was reported by investigators at Wyeth

Research[79] that the average difference between the calculated and measured  $\log P_{ow}$  values for 70 commercial drugs is about 1.05 log units.

Recently, our group has developed a high-throughput phase-distribution method based on partition of the analyte between a polymer phase and an aqueous phase in a 96-well format. The polymer phase is composed of poly (vinyl chloride) (PVC) and dioctyl sebacate (DOS) at the ratio of 1:2 (w/w). Studies in our group[48] on the correlation of polymer/water partition coefficient  $\log P_{pw}$  and standard 1-octanol/water partition coefficient ( $\log P_{ow}$ ) have shown a good linear relationship with the slope of 0.933 and the intercept close to zero, indicating that DOS plasticized PVC had lipophilicity similar to octanol. Therefore, our polymer/water partition coefficient can be used to predict lipophilicity. This method has been applied to screen chiral selectors[64] and to measure binding constants of drug-cyclodextrins inclusion complexes[80].

In this paper, we have first applied our method to determine  $pK_a$  and lipophilicity of a drug-like compound 2H-1, 2, 6-thiadiazine, 3-methyl-5-phenyl-, 1, 1-dioxide (Figure 3.1). Compounds with the 2H-1, 2, 6-thiadiazine-1, 1-dioxide substructure are prominently featured in patent and medicinal chemistry as hepatitis C virus (HCV) polymerase inhibitors[81], non-nucleoside HIV-1 reverse transcriptase inhibitors[82], analgesics[83], and smooth muscle relaxants[84]. We have further used this high-throughput method to screen lipophilicity of a library of twenty-four novel drug-like compounds. Their  $\log D_{pw}$  values (at pH 4.0, 7.0, 10.0) can be measured with good reproducibility in a high-throughput and automated format. We have found that there is a relatively poor correlation between those experimental values and calculated values with various methods.

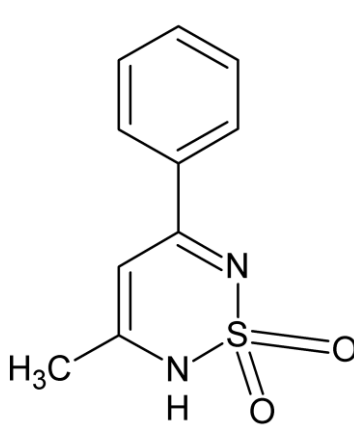


Figure 3.1 Chemical structure of 2H-1, 2, 6-thiadiazine, 3-methyl-5-phenyl-, 1, 1-dioxide.

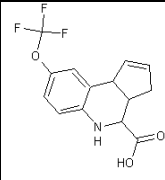
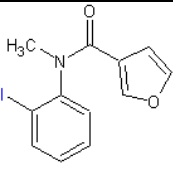
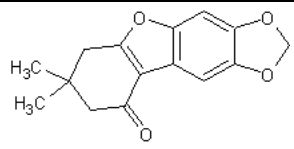
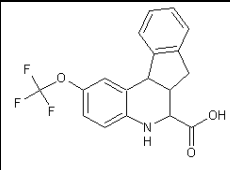
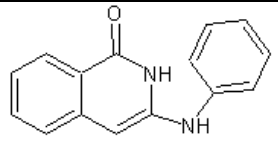
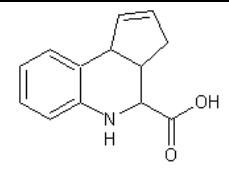
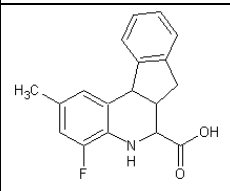
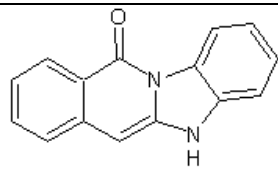
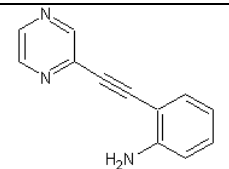
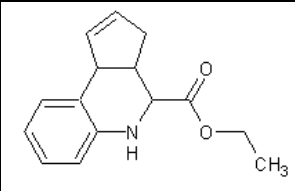
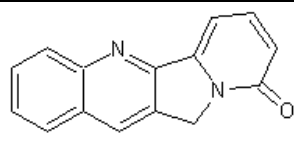
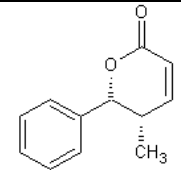
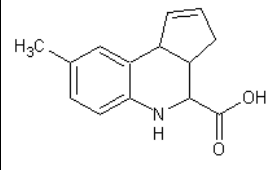
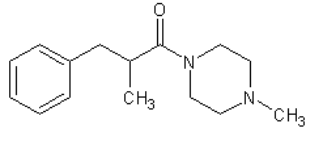
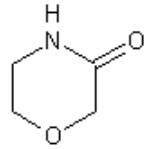
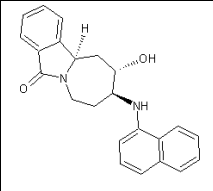
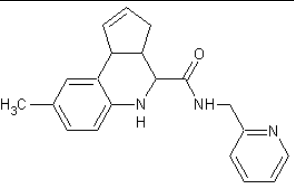
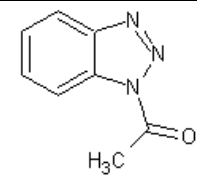
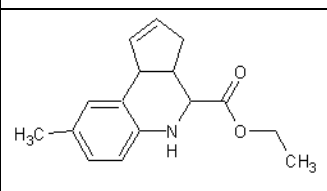
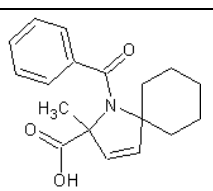
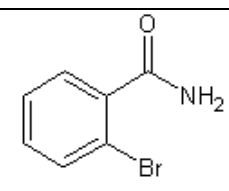
## 3.2 EXPERIMENTAL

### 3.2.1 Materials

Acetonitrile (HPLC grade), tetrahydrofuran (THF) (HPLC grade) and dimethyl sulfoxide (DMSO) (anhydrous, 99.9%) were purchased from Aldrich (Milwaukee, WI). PVC (high molecular weight) and dioctyl sebacate (DOS) were purchased from Fluka (Ronkonkoma, NY). HPLC grade trisodium phosphate, phosphoric acid, trifluoroacetic acid (TFA) were also purchased from Fluka (Ronkonkoma, NY). Water used in all the experiments was purified with a Milli-Q Synthesis A10 system (Millipore, Bedford, MA). Costar polypropylene 96-well microplates (flat bottom, 330- $\mu$ L well volume) were purchased from Fisher Scientific Co. (Pittsburgh, PA). Storage plate cap strips were purchased from Thermo Scientific Co. (Waltham, MA). 2H-1, 2, 6-thiadiazine, 3-methyl-5-phenyl-, 1, 1-dioxide and a library of twenty-four drug-like compounds were synthesized in the University of Pittsburgh Center for Chemical

Methodologies and library Development (UPCMLD) (Pittsburgh, PA). See Table 3.1 and 3.2 for structures and PubChem SID numbers.

**Table 3.1 Experimental Design of 24 compounds in a 96-well microplate**

|          | Wells 1-4   | Wells 5-8   | Wells 9-12  |
|----------|---|---|---|
| <b>A</b> |    |    |    |
| <b>B</b> |    |    |    |
| <b>C</b> |    |    |    |
| <b>D</b> |   |   |   |
| <b>E</b> |  |  |  |
| <b>F</b> |  |  |  |
| <b>G</b> |  |  |  |

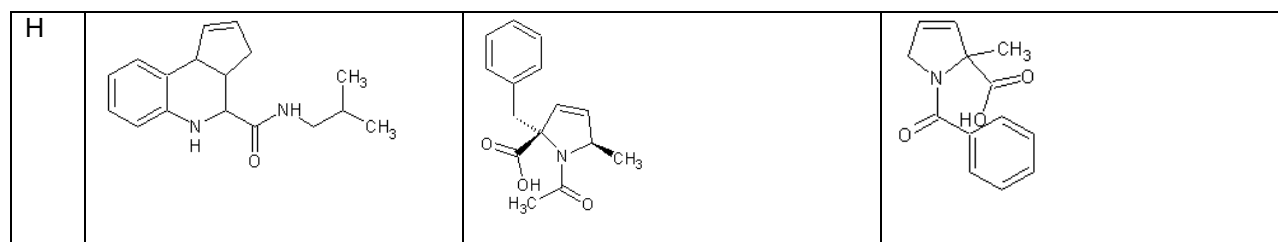


**Table 3.2 PubChem SID of 24 compounds in a 96-well microplate**

|   | Wells 1-4 | Wells 5-8 | Wells 9-12 |
|---|-----------|-----------|------------|
| A | 26696971  | 26681202  | 17390303   |
| B | 26696976  | 26683722  | 26696997   |
| C | 26696951  | 26683740  | 26681305   |
| D | 26696995  | 8142836   | 26681407   |
| E | 26696950  | 8142904   | 26681268   |
| F | 87341695  | 26696959  | 26681269   |
| G | 26696948  | 8143072   | 26681280   |
| H | 26697001  | 8143105   | 8143071    |

### **3.2.2 Equipment**

An UltraSpense 2000 microplate dispenser (KD Scientific, Holliston, MA) was used to prepare polymer films in 96-well plates. A Deep Well Maximizer (or BioShaker) (Model: M BR-022 UP, made by Taitec, Japan, and distributed by Bionexus, Inc., Oakland, CA) was used to speed up the solute distribution kinetics and control temperature. An HT-4X evaporator (Genevac inc., Gardiner, NY) was used to evaporate organic solvents. An X-LC (Jasco, Inc.) UHPLC system was used to determine the solute concentration with a UHPLC C<sub>18</sub> column (1.0 × 50 mm, particle size: 1.7 μm, Waters, Milford, MA). UV absorbances of solutes were acquired with a SpectraMax M2 microplate reader (Molecular Devices, Sunnyvale, CA) in UV-transparent microplates.

### **3.2.3 Buffer Preparation**

The phosphate-citrate buffer solutions (20 mM, pH 2.7, 2.8, 3.2, 3.9, 4.0, 5.1, 6.1, 7.0, 7.2) were made by mixing appropriate amounts of 20 mM sodium phosphate dibasic solution and 10 mM citric acid solution. The phosphate buffer solutions (20 mM, pH 1.9, 2.5, 9.2, 10.0) were made by mixing appropriate amounts of 20 mM trisodium phosphate solution and 20 mM phosphoric acid solutions. The trifluoroacetic acid (TFA) buffer solutions (pH 0.9, 1.1) were made by preparing 0.2%, 0.1% TFA in water (v/v) respectively.

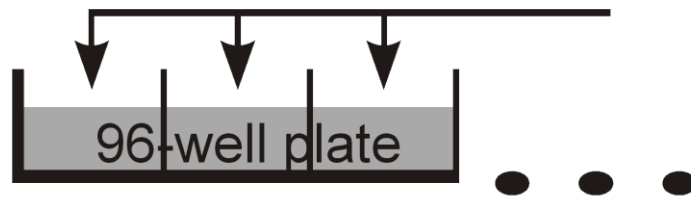
### 3.2.4 Determination of $\log P_{pw}$ and $pK_a$ of a Solute

Figure 3.2 gives the sequence of operations for  $P_{pw}$  and  $pK_a$  determination of a solute. The plasticized PVC films were prepared in polypropylene 96-well microplates. Aliquots of the solute in the aqueous buffers (200  $\mu$ L) with different pH values were then manually dispensed over the films with a multichannel pipet. The wells in each plate were covered by storage plate caps and the plate was incubated in a shaker (500 rpm, 25  $^{\circ}$ C). In order to determine the equilibration time, a kinetic study was first performed. The concentration of solute remaining in the aqueous phase was measured as a function of time. All of the other data generated were from systems at equilibrium. To determine the drug concentration, the supernatant from each well was transferred to another plate. Concentrations can be determined either by UHPLC or by measuring the absorbance in a UV plate reader. The distribution coefficient at a specific pH could be calculated as

$$D_{pw}^{pH} = \frac{(C_S - C_E) \cdot \Phi}{C_E} \quad \text{Equation 3.1}$$

Here  $D_{pw}^{pH}$  is the distribution coefficient of the solute in the polymer phase over the aqueous phase at a specific pH value.  $C_S$  is the initial solute aqueous concentration,  $C_E$  is the solute's aqueous concentration at equilibrium after the extraction, and  $\Phi$  is the phase ratio (aqueous over polymer).

Add polymer/plasticizer in THF

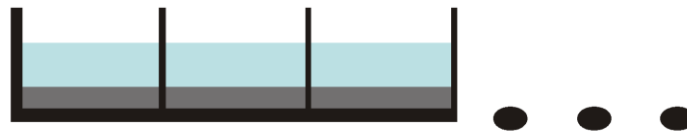


Evaporate organic solvents



Add aqueous buffer solution

Equilibrate (const. T)



Transfer the aqueous phase

Measure solute concentration  
by HPLC/plate reader

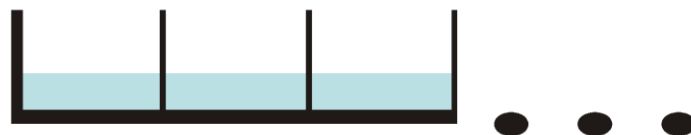


Figure 3.2 Schematic of the preparation and use of polymer films in 96-well plates for  $\text{Log } D_{pw}$  determination.

### **3.2.5 UHPLC Method to Determine Concentrations of the Thiadiazine**

A Waters UHPLC C18 column was used for this method. The mobile phase was acetonitrile-ammonium acetate buffer (pH 4.92; 10 mM) (20:80, v/v), with a flow rate of 0.1 mL/min. The back-pressure was approximately 4300 psi. The injection volume was 2  $\mu$ L. Detection was by UV absorbance at 343 nm, at which the solute peak had best signal-to-noise ratio. Peak area was used for the calibration and determination of sample concentration. The time per analysis was  $\sim$ 1.3 min.

### **3.2.6 UV Plate Reader Method to Determine Concentrations of the Thiadiazine**

UV absorbances of the solute at 343 nm were used for calibration and determination of solute concentrations. They were acquired with a microplate reader in UV-transparent 96-well plates. Absorbances of the buffers were measured as the background and subtracted to get the absorbances of the solute.

### **3.2.7 Lipophilicity Screening of the Library**

Ten nmol of 24 compounds in 20  $\mu$ L DMSO were placed in a 96-well microplate according to the experimental design shown in Table 3.1. The PubChem SID numbers of those compounds are shown in Table 3.2. According to the experimental design shown in Figure 3.2, a THF solution of plasticizer and PVC was then dispensed into the plate, which was gently shaken for a few minutes to let the compound and the polymer dissolve in THF/DMSO mixed solvent. An evaporator was then used to evaporate THF and DMSO, leaving homogeneous polymer films

with dissolved solutes formed at the bottom of the wells. Aliquots of the aqueous buffer solutions (pH 4.0, 7.0, 10.0) were then dispensed on top of the polymer films in the plate. The plate was covered and incubated in a shaker (500 rpm, 25 °C) for 4 hours. To determine the solute concentration, the supernatant from each well was transferred to another UV-transparent plate by a multichannel pipet and put in the plate reader for UV determination at 250 nm, at which sample peaks showed the best signal-to-noise ratios. If all of the solute was extracted into the 100  $\mu\text{L}$  of aqueous phase, the solute concentration in the aqueous buffer would be 100  $\mu\text{M}$ .

### 3.3 RESULTS AND DISCUSSION

#### 3.3.1 Theories to Determine Partition Coefficient and $pK_a$ of a Solute simultaneously

2H-1, 2, 6-thiadiazine, 3-methyl-5-phenyl-, 1, 1-dioxide is a weakly acidic amide due to its sulfonamide group. It will be largely ionized in an environment having pH larger than its  $pK_a$ . In practice not only neutral molecules but also ion pairs may partition. The distribution of the neutral and the ionized form between the polymer film phase and the aqueous phase is determined by the distribution coefficient  $D_{pw}$ :

$$D_{pw} = \frac{[S^-]_{film} + [HS]_{film}}{[S^-] + [HS]} \quad \text{Equation 3.2}$$

Where  $[HS]$  and  $[HS]_{film}$  are the drug concentrations in the aqueous phase and film phase, respectively;  $[S^-]$  and  $[S^-]_{film}$  are the concentrations of the ionized drug and its ion pair in the aqueous phase and film phase. The partition coefficient for the neutral drug is defined as:

$$P_{pw} = \frac{[HS]_{film}}{[HS]} \quad \text{Equation 3.3}$$

The partition coefficient for the anionic drug and its ion pair is defined as:

$$P_{pw}^- = \frac{[S^-]_{film}}{[S^-]} \quad \text{Equation 3.4}$$

It is known that the equilibrium equation for acid dissociation constant  $K_a$  is

$$K_a = \frac{[S^-]_{Aq}[H^+]}{[S]_{Aq}} \quad \text{Equation 3.5}$$

Inserting Equation (3.3), (3.4), and (3.5) into Equation (3.2):

$$D_{pw} = \frac{P_{pw} + P_{pw}^- \cdot \frac{[S^-]}{[HS]}}{1 + \frac{[S^-]}{[HS]}} = \frac{P_{pw} + P_{pw}^- \cdot \frac{K_a}{[H^+]}}{1 + \frac{K_a}{[H^+]}} = P_{pw}^- + \frac{P_{pw} - P_{pw}^-}{1 + 10^{pH - pK_a}} \quad \text{Equation 3.6}$$

By plotting  $D_{pw}$  versus pH, the  $P_{pw}$ ,  $P_{pw}^-$  and  $pK_a$  values of the solute can be obtained by applying a nonlinear least-squares curve fitting according to Equation (3.6).

### 3.3.2 Determination of $\log P_{pw}$ and $pK_a$ of a solute in a 96-well format

A kinetic study was first performed to determine the time needed for the phase distribution of the solute to reach equilibrium. The results show that 2 h were enough for the distribution experiments to reach equilibrium. Based on the kinetic data, all other distribution experiments were performed for 4 h.

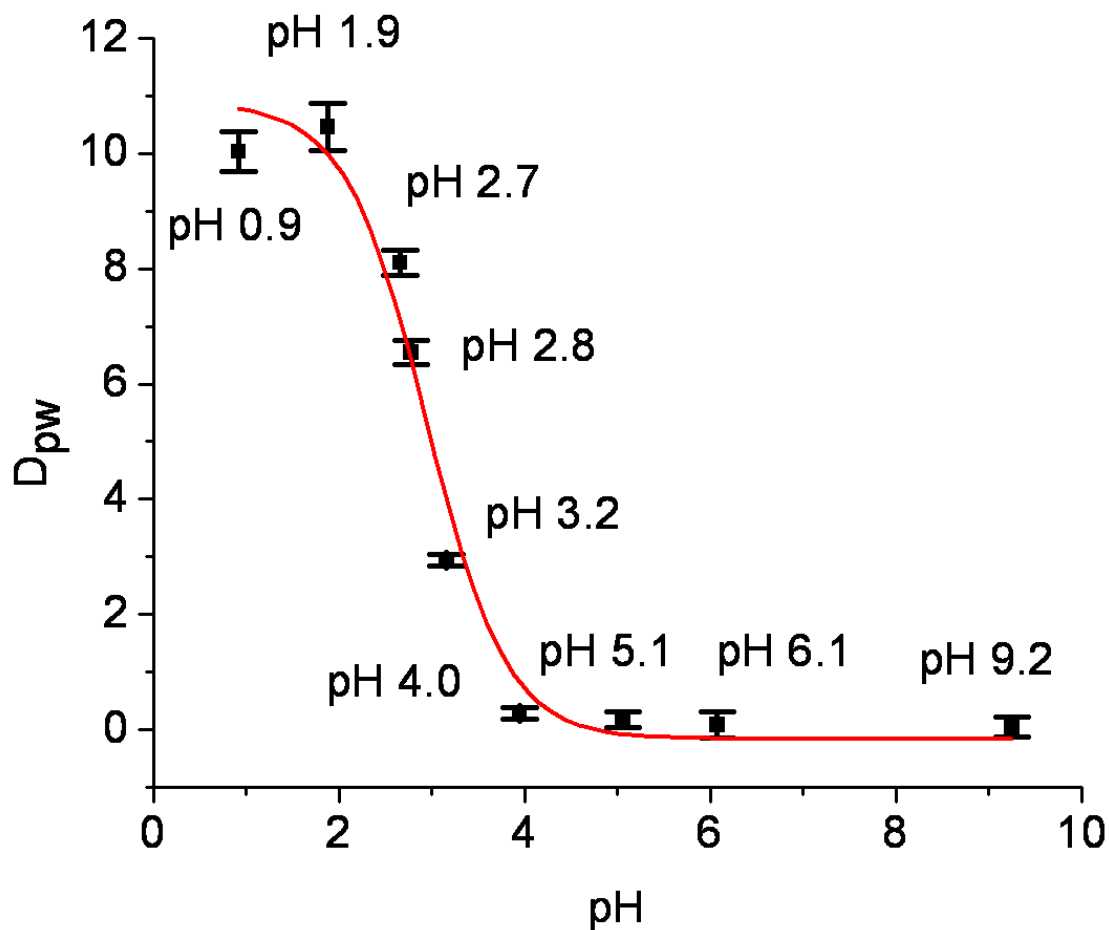
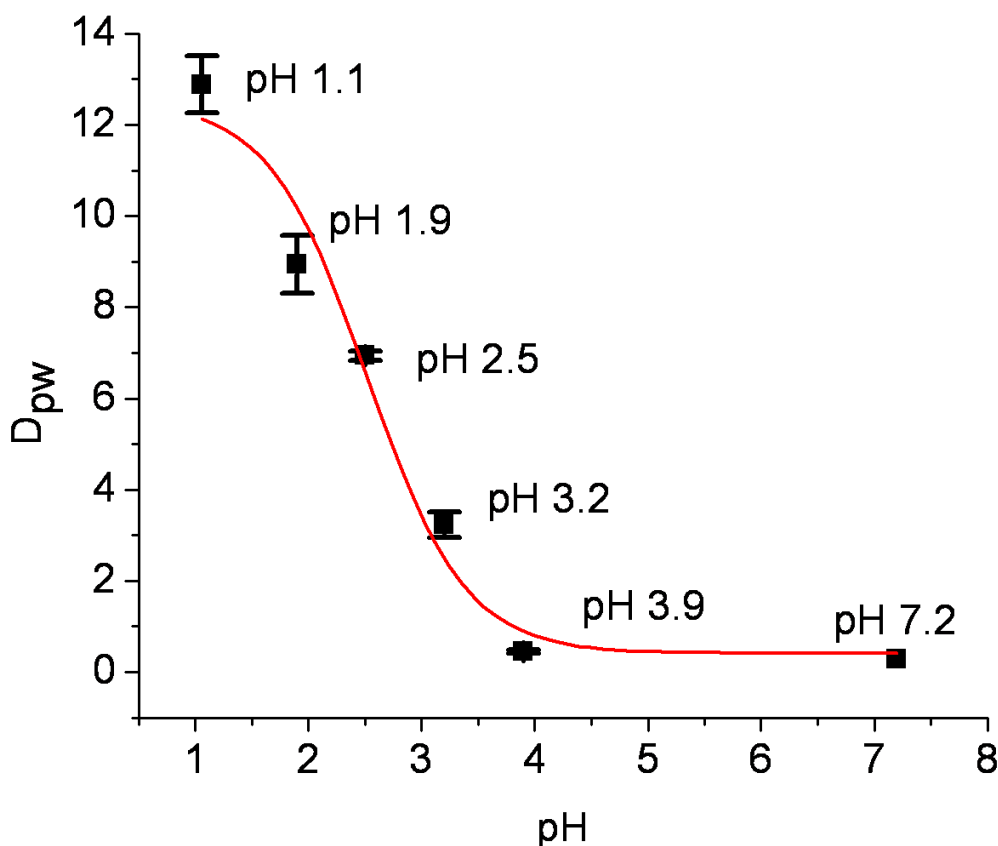


Figure 3.3 Distribution coefficients of 2H-1, 2, 6-thiadiazine, 3-methyl-5-phenyl-, 1, 1-dioxide at various pH values analyzed by UHPLC.



**Figure 3.4 Distribution coefficients of 2H-1, 2, 6-thiadiazine, 3-methyl-5-phenyl-, 1, 1-dioxide at various pH values determined by plate reader.**

Distribution coefficients of the compound, 2H-1, 2, 6-thiadiazine, 3-methyl-5-phenyl-, 1, 1-dioxide were determined at various pH values, analyzed by both UHPLC and UV plate reader. The results obtained by UHPLC and plate reader are shown in Figure 3.3 and 3.4 respectively. Each measurement was repeated twice and the corresponding error bars indicate the standard error of the mean (SEM). The SEM values were then used in error propagations to determine the errors of the calculated distribution coefficients. It is shown that distribution coefficient of the compound decreases with increasing pH of the buffer, indicating more ionic form existing in the

higher pH range, which is consistent with the fact 2H-1, 2, 6-thiadiazine, 3-methyl-5-phenyl-, 1, 1-dioxide is an acidic amide. Applying nonlinear least-squares curve fitting based on Equation (3.6), the  $P_{pw}$ ,  $P_{pw}^-$  and  $pK_a$  values of the solute were obtained. The  $pK_a$  values of the solute are  $2.94 \pm 0.10$  and  $2.52 \pm 0.17$ , determined by HPLC and plate reader measurements of the equilibrium concentration of the solute in the aqueous phase respectively. The  $\log P_{pw}$  values are  $1.04 \pm 0.02$  and  $1.10 \pm 0.03$  respectively. Both of the  $P_{pw}^-$  values are statistically zero ( $p > 0.05$ ), indicating most of the ionized solute stays in the aqueous phase rather than the polymer film phase.

To our knowledge, there have been no reported experimental  $\log P$  and  $pK_a$  values for 2H-1, 2, 6-thiadiazine, 3-methyl-5-phenyl-, 1, 1-dioxide. Compared to the calculated  $\log P_{ow}$  ( $1.10 \pm 0.75$ ) using ACD software (Advanced Chemistry Development inc., Toronto, Canada), our results are consistent and showed better precision. The calculated  $pK_a$  value from ACD software and ADMET Predictor<sup>TM</sup> software (Simulations Plus inc., Lancaster, CA) are 5.13 and 0.25 respectively, which are quite different from each other, while our results are in the middle. 2H-1, 2, 6-thiadiazine, 3-methyl-5-phenyl-, 1, 1-dioxide is a tautomeric and ionizable compound with both acidic and basic centers. It is known that predictions are not particularly good for partition coefficients and  $pK_a$  values of zwitterionic, tautomeric and charged compounds[78]. The UHPLC method gives better sensitivity than the optical absorbance measurements[48]. Unlike the plate reader method, it does not suffer from the potential for interfering compounds biasing the result. The higher sensitivity translates into the method's capability to measure a wider dynamic range of  $\log P_{pw}$  values in comparison to the optical absorbance approach [10]. On the other hand, compared to the plate reader, the UHPLC measurement generates lower throughput due to method development time. Thus both approaches have strengths. For detailed

analysis of a single compound, the UHPLC method may be better, but for screening large numbers of dissimilar compounds, the optical absorbance method is preferred unless the molar absorptivities of the solutes are too low.

### 3.3.3 Optical Absorbance-based Lipophilicity Screening of a Library of Drug-like Compounds

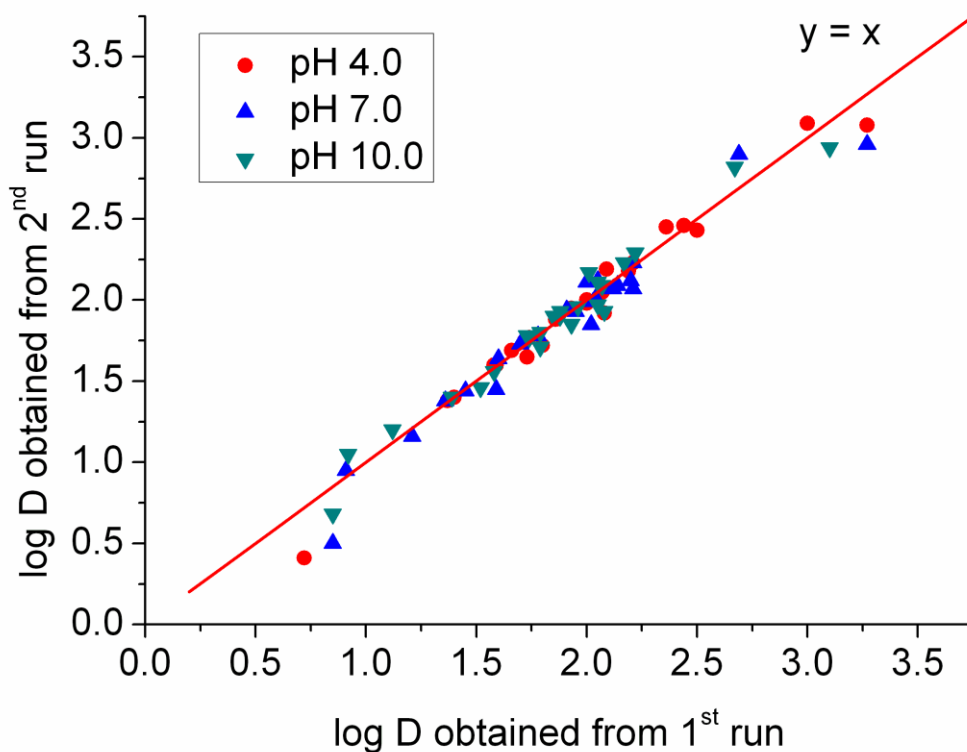


Figure 3.5 Correlation of distribution coefficients between different runs.

The experimental  $\log D$  results (pH 4.0, pH 7.0, and pH 10.0) of all of these compounds have been successfully obtained. As shown in Figure 3.5, good linearity was found for a plot of  $\log D$  for each compound in separate runs with a correlation coefficient of 0.97. A slope of 1.00

$\pm 0.05$  and an intercept of  $-0.04 \pm 0.10$  ( $p > 0.05$ , statistically zero) was found, showing good reproducibility of our method. The experimental  $\log D_{\text{pH}7.0}$  results are located in the range of 0.68 to 3.12. According to Lipinski's rule of five[85,86], drug-like molecules should have  $\log D$  values less than five for reasonable absorption and permeation. These compounds have appropriate  $\log D$  values to be considered as drug-like compounds. Errors in the quantitative determination of solute concentrations contributed to the limits for the applicable  $\log D$  range of our method. For example, if the  $\log D$  value is equal to -1 at the phase ratio equal to 16, the final concentration after the extraction would be 99.4% of the initial concentration calculated from Equation (3.1), meaning the error could not be higher than  $\pm 0.3\%$ , which is not easy to achieve with optical absorbance. Therefore, the measurable  $\log D$  range of our method is three units at one fixed phase ratio. Of course, it is easy to alter the phase ratio by changing the volume of the aqueous phase and the polymer phase. For example, this method successfully measured the lipophilicity of the hydrophobic drug econazole ( $\log P = 4.83$ )[48]. This is a challenge for the shake-flask method.

Compared to other experimental methods, this method shows several advantages. The technique is faster, more automated, and compatible with microplates unlike the standard shake-flask method. This method also demonstrates capability of determining  $\log D$  for charged compounds which is a challenge for the RPLC method.

Our experimental results and calculated  $\log D$  values by MarvinView software (ChemAxon Ltd., Budapest, Hungary) and the correlation are represented in Table 3.3 and Figure 3.6 respectively. There were rather poor correlations between measured ( $y$ ) and calculated ( $x$ )  $\log D$  values with  $y = 1.86 + 0.08 * x$  ( $r = 0.16$ ),  $y = 1.64 + 0.19 * x$  ( $r = 0.50$ ),  $y = 1.79 + 0.11 * x$  ( $r = 0.37$ ), for pH 4.0, 7.0, and 10.0 respectively. The average difference between the calculated

and measured values is 1.04 log units, which is similar to the reported difference (1.05 log units) for 70 commercial drugs[79]. Computational approaches will always be approximate because new compounds may contain substructures that are not covered by the software. Therefore, an accurate contribution of each substructure of the new compounds may not exist. Moreover, it is known that theoretical predictions are not reliable for distribution coefficients and  $pK_a$  values of zwitterionic, tautomeric and charged compounds[78], like most of the compounds in this library.

**Table 3.3 Experimental and calculated log *D* results for 24 compounds at pH 4.0, 7.0, 10.0**

| Wells | pH 4.0   |            | pH 7.0   |            | pH 10.0  |            |
|-------|----------|------------|----------|------------|----------|------------|
|       | Measured | Calculated | Measured | Calculated | Measured | Calculated |
| A 1-4 | 1.87     | 1.82       | 1.62     | 0.28       | 1.80     | -0.55      |
| B 1-4 | 3.04     | 3.34       | 2.79     | 3.34       | 2.75     | 1.10       |
| C 1-4 | 2.47     | 3.38       | 0.93     | 0.87       | 0.99     | -0.21      |
| D 1-4 | 2.21     | 2.39       | 2.22     | 2.39       | 2.21     | 2.39       |
| E 1-4 | 1.40     | 1.55       | 1.78     | -0.16      | 1.88     | -1.47      |
| F 1-4 | 2.00     | 2.56       | 2.01     | 2.72       | 1.96     | 2.72       |
| G 1-4 | 2.54     | 2.91       | 2.57     | 2.91       | 2.58     | 2.91       |
| H 1-4 | 2.40     | 2.55       | 2.12     | 2.55       | 2.26     | 2.55       |
| A 5-8 | 2.22     | 3.00       | 2.16     | 3.00       | 1.90     | 3.00       |
| B 5-8 | 1.60     | 2.89       | 1.94     | 2.89       | 1.75     | 2.89       |
| C 5-8 | 2.45     | 2.78       | 2.22     | 2.80       | 2.08     | 2.80       |
| D 5-8 | 1.38     | 1.78       | 1.37     | 1.83       | 1.40     | 1.83       |
| E 5-8 | 2.18     | -0.84      | 2.14     | 1.82       | 2.20     | 2.09       |
| F 5-8 | 1.75     | 2.03       | 1.94     | 2.41       | 1.89     | 2.41       |
| G 5-8 | 1.69     | 2.72       | 1.19     | 0.01       | 1.16     | -0.41      |
| H 5-8 | 1.94     | 1.33       | 1.92     | -1.40      | 1.76     | -1.91      |

|        |      |       |      |       |      |       |
|--------|------|-------|------|-------|------|-------|
| A 9-12 | 3.18 | 2.41  | 3.12 | 2.41  | 3.02 | 2.41  |
| B 9-12 | 1.76 | 1.29  | 2.01 | 0.75  | 2.01 | -1.98 |
| C 9-12 | 1.99 | 1.16  | 2.02 | 1.22  | 1.89 | 1.22  |
| D 9-12 | 2.06 | 2.97  | 2.10 | 2.97  | 2.01 | 2.97  |
| E 9-12 | 2.00 | -1.15 | 2.05 | -1.15 | 2.09 | -1.15 |
| F 9-12 | 2.14 | 0.62  | 2.09 | 0.62  | 2.08 | 0.62  |
| G 9-12 | 1.59 | 1.59  | 1.45 | 1.59  | 1.49 | 1.59  |
| H 9-12 | 0.56 | 2.72  | 0.68 | 0.01  | 0.77 | -0.41 |

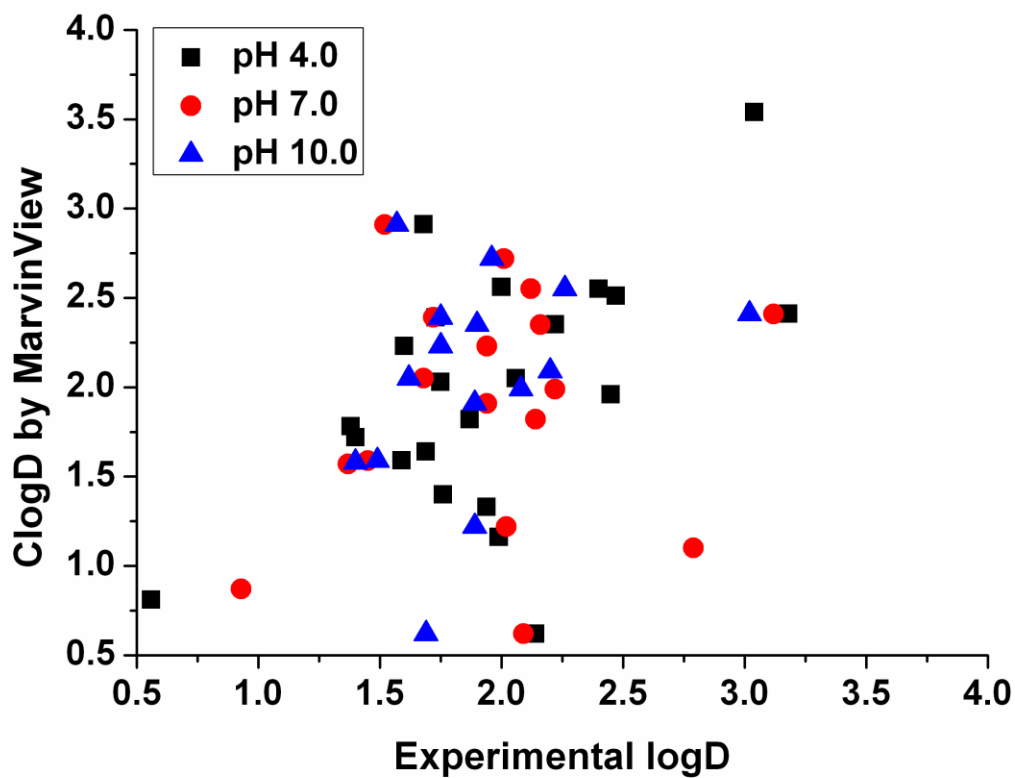


Figure 3.6 Correlation of distribution coefficients between our experimental values and calculated values.

We then compared experimental  $\log P$  values and  $\text{clog}P$  for only the neutral compounds in the library by four different software packages, ACD, Marvin, QikProp (Schrodinger, Portland, OR), and Sybyl (Tripos Inc., St. Louis, MO). As summarized in Table 3.4, a total average  $\log P$  difference of 0.58 log units are shown for neutral compounds, smaller than that for ionizable compounds. Better correlations between measured (y) and calculated (x)  $\log P$  values were shown with  $y=0.91+0.52*x$  ( $r=0.91$ ),  $y=1.31+0.31*x$  ( $r=0.43$ ),  $y=0.96+0.46*x$  ( $r=0.45$ ),  $y=0.92+0.47*x$  ( $r=0.82$ ) for ACD, QikProp, Marvin, and Sybyl respectively. We note, however, that even for neutral compounds the range of  $\text{clog}P$  values yielded by the different programs is often significant.

**Table 3.4 Experimental and calculated  $\log P$  results for 10 neutral compounds in the library.**

| Wells  | Experimental $\log P$ | ACD  | QikProp | Marvin | Sybyl | RSD% of calculated $\log P$ | Average Difference |
|--------|-----------------------|------|---------|--------|-------|-----------------------------|--------------------|
| D 1-4  | 2.21                  | 2.74 | 3.25    | 2.39   | 2.76  | 13%                         | 0.57               |
| G 1-4  | 2.56                  | 3.20 | 3.59    | 2.91   | 3.25  | 9%                          | 0.67               |
| H 1-4  | 2.26                  | 2.53 | 3.03    | 2.55   | 2.83  | 9%                          | 0.47               |
| A 5-8  | 2.09                  | 2.35 | 2.72    | 3.00   | 2.11  | 15%                         | 0.45               |
| B 5-8  | 1.76                  | 2.24 | 2.75    | 2.89   | 2.83  | 11%                         | 0.91               |
| C 5-8  | 2.25                  | 1.99 | 2.77    | 2.80   | 3.20  | 19%                         | 0.57               |
| D 5-8  | 1.38                  | 1.58 | 2.33    | 1.81   | 1.92  | 16%                         | 0.53               |
| A 9-12 | 3.11                  | 3.96 | 2.26    | 2.41   | 3.84  | 29%                         | 0.78               |
| D 9-12 | 2.06                  | 2.05 | 2.20    | 2.97   | 1.97  | 20%                         | 0.29               |
| G 9-12 | 1.51                  | 0.73 | 1.09    | 1.59   | 0.77  | 38%                         | 0.51               |

Our choice of buffer components was made based on the range of pH values and the compatibility with the analytical methods used. We also wanted to minimize the number of

buffer components use across the total range of pH values. Ultimately, we chose phosphate and phosphate/citrate which are adequate for the entire pH range investigated except near pH 10. We determined that the poor buffer capacity of phosphate at pH 10 was not a limitation. From Table 3.3, the lowest  $\log D_{\text{pH}10}$  is about -2. Using Eqn.1, the aqueous concentration for this solute would be 100  $\mu\text{M}$  at equilibrium (phase ratio = 20). The phosphate buffer concentration is 20 mM. So the solute concentration is at most 0.5% of the buffer concentration. The  $\text{p}K_{\text{a}}$  values of phosphoric acid are 2.1, 7.2, and 12.2. At pH 10,  $[\text{HPO}_4^{2-}]/[\text{PO}_4^{3-}] = 158$ . From the structures shown in Table 3.1, most of our solutes in the library are amines. If the solute has the same basic strength as NaOH, which is the worst case, 0.5% of the acidic ion will be neutralized,  $\text{pH} = 12.2 - \log(157.2/1.8) = 10.26$ . The small change of pH will not influence the measured distribution coefficient unless the  $\text{p}K_{\text{a}}$  of the solute is around 10. In that case, only about half of the solute can neutralize the acidic ion in the buffer (0.25%),  $\text{pH} = 12.2 - \log(157.6/1.4) = 10.15$ . In conclusion, despite the phosphate buffer's low strength at pH 10.0 distribution coefficients will be measured accurately in our experiment because of the solute and buffer concentrations used.

### 3.4 CONCLUSIONS

We have successfully developed a phase-distribution method to measure simultaneously  $\text{p}K_{\text{a}}$  and lipophilicity of drug-like compounds using well-plate technologies. This method has been applied successfully to measure  $\text{p}K_{\text{a}}$  and  $\log P_{\text{pw}}$  values of a drug-like compound, 2H-1, 2, 6-thiadiazine, 3-methyl-5-phenyl-, 1, 1-dioxide. Moreover, the distribution coefficients of a library of novel drug-like compounds were determined by this approach. This method is fast,

requires only a small amount of material, has great flexibility, and has the potential to be fully automated; thus showing great potential in the pharmaceutical and environmental fields.

## **4.0 FLUOROUS RECEPTOR-FACILITATED SOLID PHASE MICROEXTRACTION**

This chapter has been published in *J. Chromatogr. A* (DOI:10.1016/j.chroma.2014.07.060).

Reproduced with permission from *J. Chromatogr. A*. Copyright (2014) Elsevier.

### **4.1 INTRODUCTION**

Sample preparation is an essential step in the analysis process. Solvent-free extraction is considered to be a green analytical method as it prevents hazards to the environment and human health. Solid phase microextraction (SPME) is a widely accepted solvent-free extraction technique that usually uses a polymer sorbent as the extraction phase. Various configurations of SPME have been considered to date, including coated fibers and vessels[3].

The selection of sorbent polymer material is the most important step controlling the selectivity of the extraction[8]. One of the recent trends in SPME is to study new coatings with higher extraction efficiency and selectivity[9]. Recently developed coatings for selective extraction include molecularly imprinted polymers (MIP)[10-17], ionic liquids[19-23], metal complexes[24], and carbon nanotubes[25,26]. We showed some time ago that a molecular receptor for barbiturates embedded in the extraction phase enhances the selectivity of SPME for barbiturates that bind well to the receptor[87]. Such receptors are potentially very powerful tools for selective extractions by taking advantage of noncovalent bonding between a receptor and an

analyte. However, while receptors can improve selectivity by augmenting the distribution coefficient of the selected analytes, the matrix in which the receptor resides plays a role as well. Ideally, the matrix would decrease the distribution coefficient for uninteresting analytes while the receptor increases the distribution coefficient of interesting analytes. This notion guided us to fluorinated solvents and materials as potential matrices for SPME.

Fluorinated solvents are the least polar practical solvents known[88]. Fluorinated liquids are virtually immiscible with both aqueous and most organic phases. Due to their extreme nonpolar character, noncovalent associations including hydrogen bonding tend to be enhanced in fluorinated media[89]. Molecular recognition has been combined with fluorinated matrices to improve extraction selectivity by reducing the interfering species extracted. Palomo et al. reported that the fluorinated solubility of fluorinated N, N'-dialkylureas could be enhanced by embedding perfluoroalkanoic acids in perfluorohexanes (FC-72) due to formation of hydrogen bonded complexes[90]. O'Neal and coworkers also reported that a carboxylic acid terminated polyhexafluoropropylene oxide, Krytox 157 FSH (**1**), significantly enhances the extraction of pyridines from chloroform into FC-72 by forming a hydrogen bond between the pyridine ring and the carboxylic acid group[91].

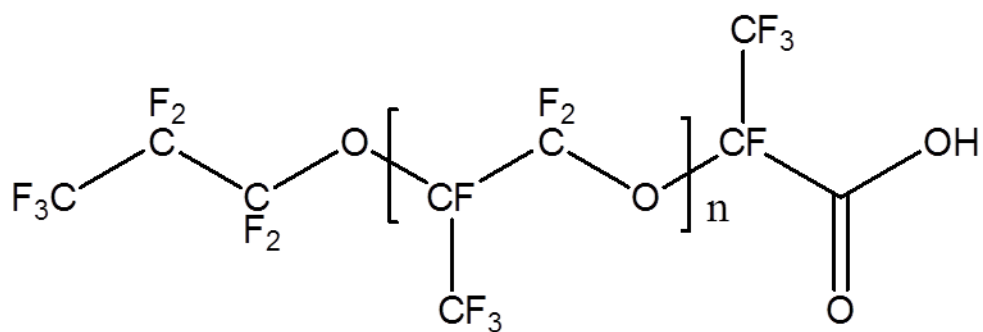
Teflon AF 2400 (**2**) is a chemically inert and thermally stable amorphous fluorinated polymer. It is a copolymer of tetrafluoroethylene (13%) and 2, 2-bis(trifluoromethyl)-4, 5-difluoro-1, 3-dioxole (87%)[92]. Homogeneous thin films of Teflon AF 2400 are easily prepared through solvent casting[93]. They are transparent through a wide UV-Vis and IR range[94], making them ideal to study noncovalent associations. Teflon AF 2400 has a high fractional free volume (FFV) probably due to its rigid structure of the dioxolane ring and the weak van der Waals interactions between fluorinated polymeric chains[18]. Krytox 157 FSH is thermally stable

and can be easily incorporated into Teflon AF 2400 films. Krytox 157 FSH and Teflon AF 2400 were found to be miscible in any proportion[95].

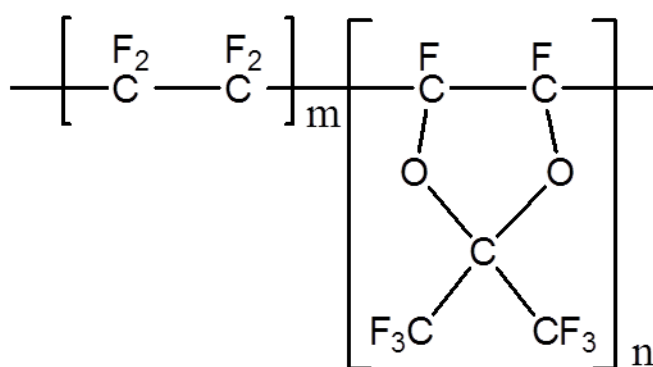
We are interested in developing receptor-doped fluoruous films for solid phase microextraction. The hydrophobic and lipophobic properties of the fluoruous films will reduce the polymer-water distribution coefficient of all solutes except the ones that can form noncovalent interaction with the fluoruous receptor, making extractions selective.

We recently reported a 96-well parallel design to measure distribution coefficients of novel drug-like compounds between a plasticized polyvinyl chloride (PVC) film and an aqueous phase[96]. This parallel design is fast and only requires small amounts of sample. In this work, we have applied this parallel approach to create a 96-well vessel SPME to study distribution between receptor-doped fluoruous polymer phase and an aqueous phase. Based on previous results on hydrogen bonding of pyridine and pyridine derivatives with carboxylic acids in the fluoruous liquids[91], we chose to study the distribution behavior of quinoline (**3**), an environmental contaminant and a probable human carcinogen[97], between a fluoruous polymer phase composed of Krytox 157FSH doped Teflon AF 2400 and an aqueous phase.

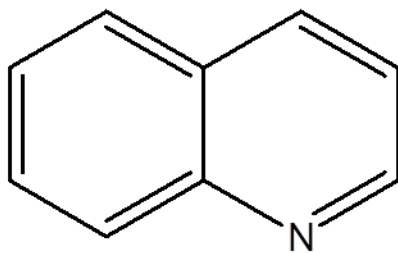
We found that the addition of a fluoruous carboxylic acid to the film increased the polymer-water distribution coefficients of the nitrogen heterocycle. We studied the effects of receptor concentration and solute concentration on the distribution coefficients based 96-well vessel SPME. We then coated this receptor doped fluoruous polymer on a stainless steel fiber for SPME. Compared to a commonly used SPME fiber made of polydimethylsiloxane (PDMS), Krytox 157-FSH doped Teflon AF 2400 showed a preference for the nitrogen heterocyclic compound over a non-heterocyclic control, phenol. To our knowledge, this is the first reported receptor-doped fluoruous SPME.



1



2



3

Figure 4.1 Structure of Ktytox 157 FSH (1), Teflon AF 2400 (2), quinoline (3)

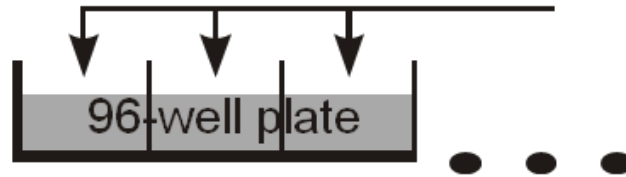
## 4.2 EXPERIMENTAL

### 4.2.1 Chemicals and Solutions

Quinoline and tris (hydroxymethyl) aminomethane hydrochloride buffer substance (Tris buffer) were obtained from Aldrich (Milwaukee, WI). Phenol and nitric acid were bought from EM Science (Cherry Hill, NJ). Krytox 157FSH was purchased from Miller-Stephenson Chemical Co., Inc. (Danbury, CT) with a number averaged molecular weight of 5150 g/mol based on an average of 29 polymer repeat units determined by  $^{19}\text{F}$ -NMR[98]. Teflon<sup>®</sup> AF 2400 was purchased from DuPont (Wilmington, DE). Fluorinert FC-72 (a mixture of perfluorohexanes) was purchased from 3M (St. Paul, MN). Aqueous tris(hydroxymethyl)aminomethane buffer (tris buffer hereafter) solutions (50.0 mM, pH = 8.0) were prepared by dissolving tris buffer pH 8.0 substance (Sigma Aldrich, Milwaukee, WI) in purified water (Milli-Q water) from a Millipore Synthesis A10 system (Millipore, Billerica, MA). Quinoline and phenol solutions with a variety of concentrations were prepared in this tris buffer.

#### 4.2.2 96-well Vessel SPME: Preparation and Extraction

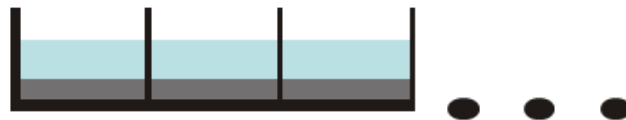
Add Teflon AF/Receptor in FC-72



Evaporate FC-72



Add Solute Aqueous Solution  
Equilibrate (const. T)



Transfer the Aqueous Phase  
Measure Solute Concentration  
by UV Plate Reader

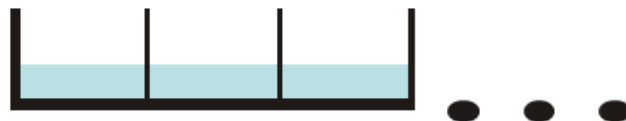


Figure 4.2 General procedure for 96-well vessel SPME.

As outlined in Figure 4.2, receptor-doped fluoros polymer films were prepared in Costar polypropylene 96-well microplates (flat-bottom, 330  $\mu\text{L}$  well volume). Both Teflon AF 2400 and Krytox 157FSH were initially prepared in FC-72 at a concentration of 10 mg/mL. These solutions were combined to give 200  $\mu\text{L}$  of a solution that would yield films with ratios of 0.0%, 12.5%, 25%, 37.5%, 50%, 75%, 100% (w/w) Krytox. Final film weights are therefore 2.0 mg. After the polymer films were formed, 200  $\mu\text{L}$  aliquots of the aqueous solute-containing films solutions were added to undivided wells. Plates were sealed by a cover and equilibrated in a shaker (BioShaker MBR-022U, made by Taitec and distributed by Bionexux Inc., Oakland, CA) at 500 r/min at 25.0  $^{\circ}\text{C}$ . In order to determine the necessary equilibration time, the percentage of quinoline extracted into the polymer phase was measured as a function of time. Other than in this experiment, all data were generated at equilibrium. After equilibrium was achieved, 100  $\mu\text{L}$  aliquots from each well were transferred into a UV-transparent microplate by a multichannel pipette. To determine the solute concentrations, UV absorbance was measured by a SpectraMax M2 microplate reader (Molecular Devices, Sunnyvale, CA). The distribution coefficient could be calculated as

$$D_{pw} = \frac{(C_S - C_E) \cdot \Phi}{C_E} \quad \text{Equation 4.1}$$

Here  $D_{pw}$  is the distribution coefficient of the solute in the polymer phase over the aqueous phase.  $C_S$  is the initial solute aqueous concentration,  $C_E$  is solute aqueous concentration at equilibrium after the extraction, and  $\Phi$  is the volume phase ratio (aqueous over polymer).

The volume of each film was estimated as

$$V_{film} = \frac{10\text{mg} / \text{mL} \times V_{solution}}{d_{film}} \approx 1\mu\text{L} \quad \text{Equation 4.2}$$

Here  $V_{solution}$  is the volume of the FC-72 solution used in each well and  $d_{film}$  is the density of the film, which is estimated to be 2 g/mL. In this work, 200  $\mu$ L of the FC-72 solution was dispensed in each well, so the volume of each film was about 1  $\mu$ L. The phase ratio was 200 as 200  $\mu$ L of the aqueous solution was used.

#### **4.2.3 Coated Fiber SPME-GC: Fiber Preparation, Extractions, and Desorption on GC**

The stainless steel wires were first soaked in 4 M HNO<sub>3</sub> to clean and passivate the steel. They were then rinsed with Milli-Q water and dried in the air. The exposed stainless steel fibers were then dip-coated 15 times with a Krytox 157FSH-doped Teflon AF 2400 solution (10 mg/mL) in FC-72 (0 and 50% (w/w) Krytox in Teflon AF). For each of the 15 “dips”, the fibers were immersed into the solution, then quickly removed after 2 seconds and dried in the air for 1 minute to evaporate the FC-72. Before use, each F-SPME fiber was exposed in a Thermo Focus GC inlet for conditioning at 250 °C for 30 min with a constant split flow of 60 mL/min and a split ratio of 20. Krytox 157FSH is thermally stable and does not desorb in the inlet of the gas chromatograph. The GC injection splitter was opened during the conditioning step to reduce the amount of impurities getting to the column. A commercially available SPME fiber with a polydimethylsiloxane (PDMS) coating (Sigma Aldrich, Bellefonte, PA) was used as a control to compare with those fibers with fluorinated coatings. It was used at the same conditioning and GC conditions as the Krytox doped Teflon films.

For the F-SPME extraction, the fibers were exposed to either the headspace or the liquid phase of a tris buffer solution (pH = 8.0) containing 100  $\mu$ M quinoline and 100  $\mu$ M phenol. GC conditions: were 250 °C inlet temperature, 100 °C initial oven temperature, hold 0.5 min, ramp

120 °C/min to 250 °C, hold 0.1 min, 60 mL/min split flow, split ratio = 20, in a 30 m long, 0.32 mm ID Rxi-5ms column ( $d_f = 0.25 \mu\text{m}$ ) (Restek, Bellefonte, PA).

Peak areas obtained from the integrated chromatograms were used for quantitation. The calibration curves were first carried out for both quinoline and phenol standard solutions, respectively. The amount of the compound was correlated to the corresponding peak area. Standard solutions were first prepared and injected to determine the linearity and limit of quantitation (LOQ) for quinoline and phenol. Good linearity has been observed for quinoline in the weight range of 0.33 ng (LOQ) to 25 ng, with a correlation coefficient close to unity ( $R^2 > 0.9999$ ). Good linearity has also been found for phenol in the weight range of 0.22 ng (LOQ) to 20 ng, with a correlation coefficient close to unity ( $R^2 > 0.9999$ ). Selectivity of quinoline over phenol was described as the ratio of the extracted amounts.

## 4.3 RESULTS AND DISCUSSION

### 4.3.1 96-well Vessel SPME

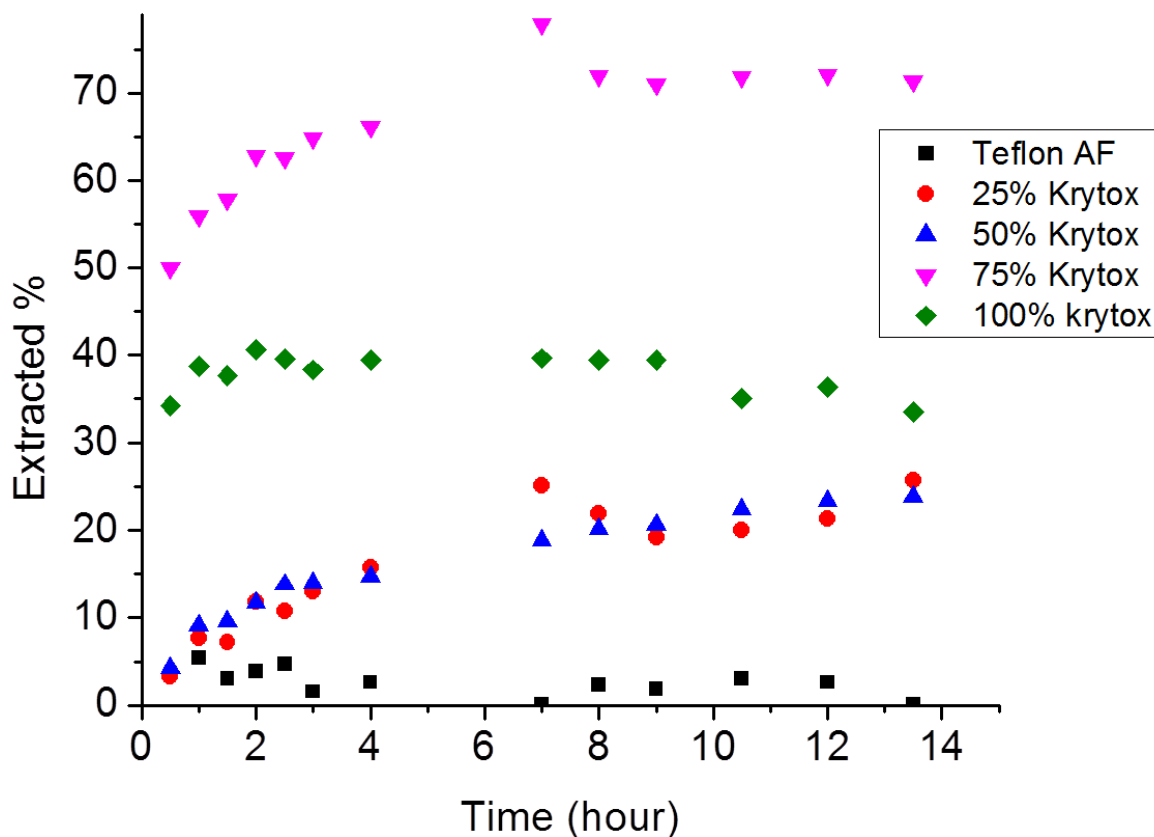


**Figure 4.3 Percentage of quinoline extracted as a function of time for Teflon AF films with different percentages of receptor doped.**

A kinetic study was first carried out to determine the time needed to reach equilibrium for the extraction of quinoline from the aqueous solution to Teflon AF films with different percentage of receptor doped. As shown in Figure 4.3, ten hours were sufficient. There was almost no extraction of quinoline into a Teflon AF film without the receptor. The equilibrium

time for that film was less than 1 hour. Based on the kinetic data, all other distribution experiments were allowed to equilibrate for ten hours.

As illustrated in Figure 4.3, the Krytox-doped Teflon AF films extract a significant percentage of quinoline from the aqueous phase, suggesting that hydrogen bonding between quinoline and the fluorinated carboxylic acid also occurs in the polymer phase as it does in a fluorinated liquid phase[91]. The data also show that the receptor concentration had an effect on the extraction efficiency.

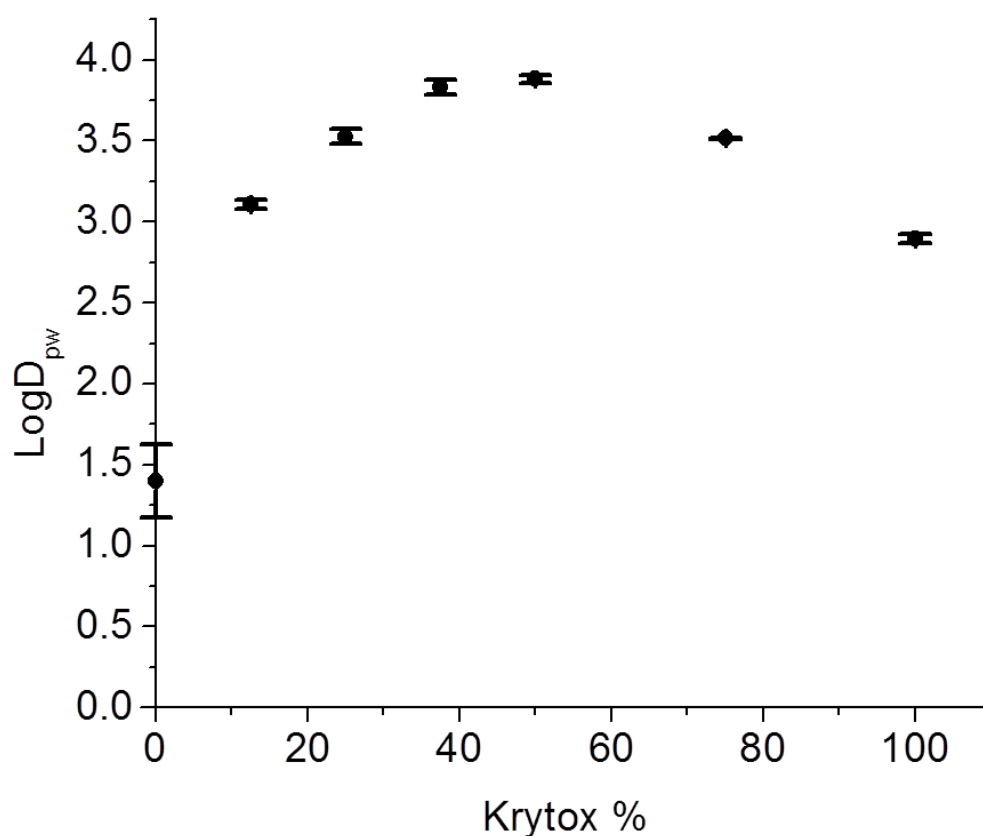


**Figure 4.4 Log  $D_{pw}$  of quinoline as a function of Krytox concentration in Teflon AF films for quinoline with an initial aqueous concentration of 50  $\mu$ M.**

We then carried out a more detailed study about the influence of the receptor concentration on the distribution coefficient. As shown in Figure 4.4,  $\log D$  of quinoline partitioning into the pure Teflon AF film is small. The polymer-water distribution coefficient of quinoline increases with higher receptor concentration in the film, but the trend is reversed when there is more than 50% (w/w) receptor in the film. Therefore, the highest polymer-water distribution coefficient appears at Teflon AF film with 50% Krytox (w/w), which corresponds to a receptor concentration of 194 mM. At this optimal concentration and at equilibrium, 97.4% of the quinoline initially in the aqueous phase was extracted into the receptor doped fluorinated film from the aqueous phase. In fact, as we describe later, the extraction is so effective that the distribution coefficient becomes dependent on the concentration of the analyte. In order to further elaborate the data, we have derived a theoretical model as below.

The distribution of the free solute between the fluorinated polymer film phase and the aqueous phase is determined by the distribution coefficient  $D_0$ :

$$D_0 = \frac{[S]_f}{[S]_{aq}} \quad \text{Equation 4.3}$$

where  $[S]_{aq}$  and  $[S]_f$  are the free solute concentration in the aqueous phase and film phase, respectively. When the receptor is added to the polymer film phase, solute and receptor forms a complex and the binding constant is defined as:

$$K_{ln} = \frac{[S \cdot L_n]_f}{[S]_f [L]_f^n} \quad \text{Equation 4.4}$$

where  $n$  is the stoichiometry,  $[L]_f$  is the free receptor concentration and  $[S \cdot L_n]_f$  is the solute-receptor complex concentration in the polymer phase. When the receptor is present in the polymer phase, the apparent solute distribution coefficient  $D_{app}$  is:

$$D_{app} = \frac{[S]_f + [S \cdot L_n]_f}{[S]_{aq}} \quad \text{Equation 4.5}$$

Dividing Equation (4.5) by Equation (4.3):

$$\frac{D_{app}}{D_0} = 1 + \frac{[S \cdot L_n]_f}{[S]_f} \quad \text{Equation 4.6}$$

After rearranging Equation (4.6) and inserting it into Equation (4.4), we obtain:

$$K_{ln} = \frac{[S \cdot L_n]_f}{[S]_f [L]_f^n} = \left( \frac{D_{app}}{D_0} - 1 \right) \cdot \frac{1}{[L]_f^n} \quad \text{Equation 4.7}$$

After converting Equation (4.7) into the logarithmic form and rearranging it, we get

$$\log \left( \frac{D_{app}}{D_0} - 1 \right) = \log K_{ln} + n \cdot \log [L]_f \quad \text{Equation 4.8}$$

The free receptor concentration in the polymer film  $[L]_f$  can be expressed as a relationship to the initial receptor concentration  $C_L$  according to mass balance:

$$[L]_f = C_L - n \cdot [S \cdot L_n]_f \quad \text{Equation 4.9}$$

After inserting Equation (4.9) into the Equation (4.8), we obtain

$$\log \left( \frac{D_{app}}{D_0} - 1 \right) = \log K_{ln} + n \cdot \log (C_L - n \cdot [S \cdot L_n]_f) \quad \text{Equation 4.10}$$

According the data in Figure 4.4, when  $[L]_f = 0$  (*i.e.*, 0% Krytox), the free solute concentration in the film,  $[S]_f$  is about  $10^{1.4}$  or 25 times higher than the aqueous concentration. The large increase in  $D_{app}$  upon addition of Krytox, up to values near  $10^4$ , is due to the formation of the complex,  $S \cdot L_n$ . Therefore, in the presence of the ligand, Krytox, the analyte in the film is mostly in the form of the complex,  $S \cdot L_n$ , the concentration of which is much larger than  $[S]_f$ . We can obtain an estimate of the binding constant and stoichiometry based on Equation 4.10 using an iteration method (Microsoft Excel Goal Seek). The stoichiometry was determined to be 1.2 and

binding constant is  $2.7 \times 10^3 \text{ M}^{-1}$ , suggesting that 1:1 complexation dominates in the polymer phase.

Quinoline and Krytox 157FSH have been reported to form 1:1, 1:2, and 1:3 complexes (base : acid) in a fluoruous liquid, FC-72[98]. The formation constant of quinoline-Krytox complex in the fluoruous polymer phase is much smaller than the reported binding constant in a fluoruous liquid, FC-72 ( $1.8 \times 10^8 \text{ M}^{-1}$ )[98]. This observation is consistent with the reported results that binding constant of Krytox and 3-hydroxypyridine complex ( $840 \text{ M}^{-1}$ ) in Teflon AF was significantly smaller than that ( $3 \times 10^6 \text{ M}^{-1}$ ) in FC-72 [27]. Although the number of data is limited, it appears that the fluoruous polymer phase and the fluoruous liquid phase are considerably different.

A pair of carboxylic acids, such as Krytox can form a cyclic dimer at high concentrations[91]. Self-association is more prevalent at high concentrations than low concentration[87]. Previous study[87] shows the similar trend as ours that self-association of a molecular receptor in poor solvent decreases its binding efficacy[87]. In our study, quinoline-receptor formation competes with the self-association of the receptor. This may explain the decreased distribution coefficient when high concentration of the receptor existed.

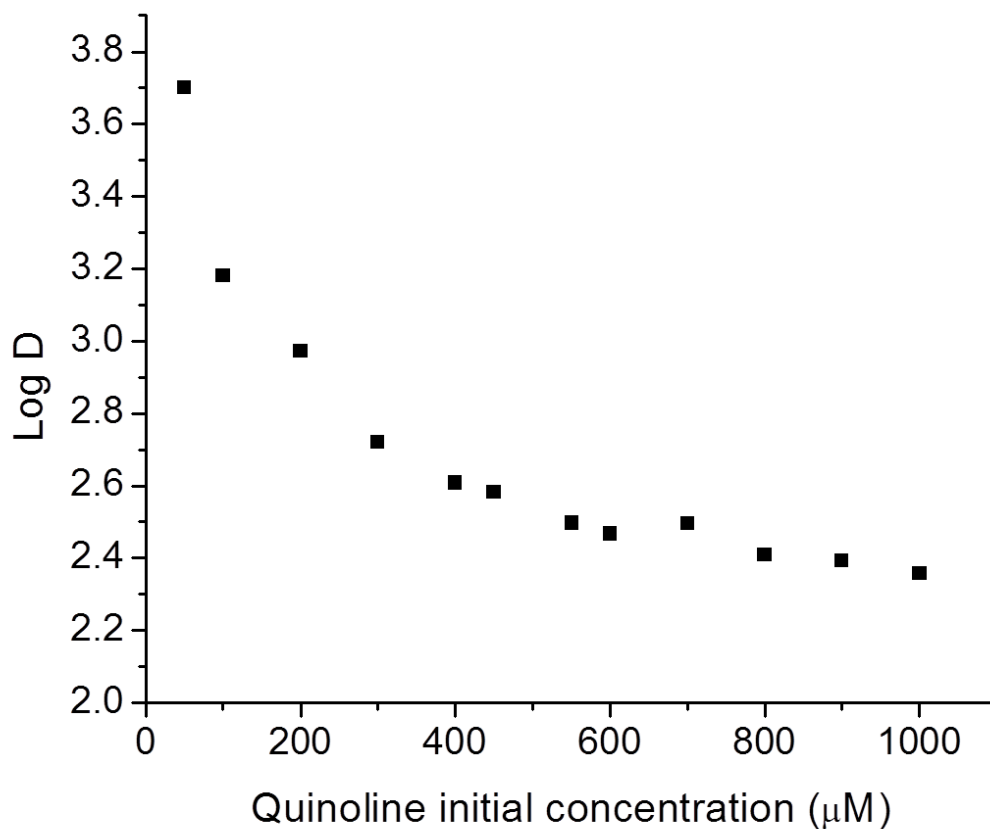


**Figure 4.5 Polymer-water distribution coefficient of quinoline as a function of the initial quinoline aqueous concentration.**

The distribution coefficient is quite large, nearly 104, with 50% Krytox. With such a large distribution coefficient based on a specific molecular interaction, it is quite possible that the distribution coefficient depends on the initial solute concentration behavior. Thus, we determined quinoline distribution behavior over a wide range of initial quinoline concentrations to determine the concentration dependence. As shown in Figure 4.5, distribution coefficient decreases as the initial quinoline concentration increases. The trend can be explained by Equation (4.10), where  $D_0$ ,  $K$ ,  $n$ , and  $C_L$  are constants in this study. The increase of quinoline initial concentration leads

to the increase of  $[S:L_n]_f$ , thus the decrease of the distribution coefficient  $D_{app}$ , which is consistent with the findings in Figure 4.5.

Selectivity of quinoline over its non-heterocyclic counterpart was studied. Phenol has been chosen as a good control because it is aromatic, it has a similar lipophilicity as quinoline but it does not contain the nitrogen. It also shows good solubility in water as well as a variety of organic solvents[99]. Importantly, the addition of fluoros carboxylic acids to fluoros liquid (FC-72), which dramatically increases pyridine distribution to the fluoros phase has no measureable effect on the distribution of phenol[91].

**Table 4.1 Distribution coefficients and selectivity for quinoline and phenol in pure Teflon AF and Teflon AF with 50% Krytox**

|             | Dpw(pure Teflon vs. Aqueous) | Dpw(Teflon+50%Krytox vs. Aqueous) |
|-------------|------------------------------|-----------------------------------|
| Phenol      | 4.5                          | 130                               |
| Quinoline   | 25                           | 7640                              |
| Selectivity | 5.5                          | 59                                |

Table 4.1 reveals the distribution coefficients of quinoline and phenol at initial solute concentration of 50  $\mu$ M in pure Teflon AF and Teflon AF with 50% Krytox. The receptor-doped Teflon AF film shows a higher selectivity, 59, for quinoline over phenol while the pure Teflon AF film without receptor only shows a selectivity of 5.5. The significant improvement on selectivity demonstrates the effective hydrogen bonding of fluoros carboxylic acid group and nitrogen heterocyclic compound in the fluoros polymer medium.

Compared to the previous reported receptor doped fluoros liquid-liquid extraction[91], this 96-well vessel SPME shows some advantages. As a green analytical method, this solvent-

free extraction technique minimizes waste and human exposure to hazardous solvents. This SPME method requires small amount of sample, and it operates in parallel.

The effects of receptor and solute concentration on the distribution coefficient and selectivity based on 96-well vessel SPME have been discussed as above. We then coated this receptor doped fluoruous polymer on a stainless steel fiber as the coated fiber SPME.

#### **4.3.2 Coated Fiber SPME**

Coated fiber SPME is the most widely used SPME configuration. SPME is usually performed by either direct extraction in the liquid phase or headspace extraction. In the direct extraction mode, the coated fiber is inserted into the sample matrix to extract analytes into the extraction phase. In the headspace extraction mode, the fiber is inserted into the gaseous headspace above the sample matrix to extract those relatively volatile analytes. In order to compare feasibility of those modes, we first exposed the SPME fiber made from 50% Krytox/Teflon AF to both the liquid phase and the headspace of aqueous quinoline solutions. The fibers were then exposed at the GC inlet where the quinoline was desorbed. The peak areas were used for quantitation. Figure 4.6 shows the effect of quinoline initial concentration on SPME extraction based on both liquid phase and headspace exposure. For liquid phase extraction, it shows a linear relationship with a correlation coefficient close to unity ( $R^2 = 0.999$ ) and a slope of 0.0259 ng/ $\mu$ M. The detection limit was calculated to be 34.9  $\mu$ M based on the standard deviation and the slope of the regression line.

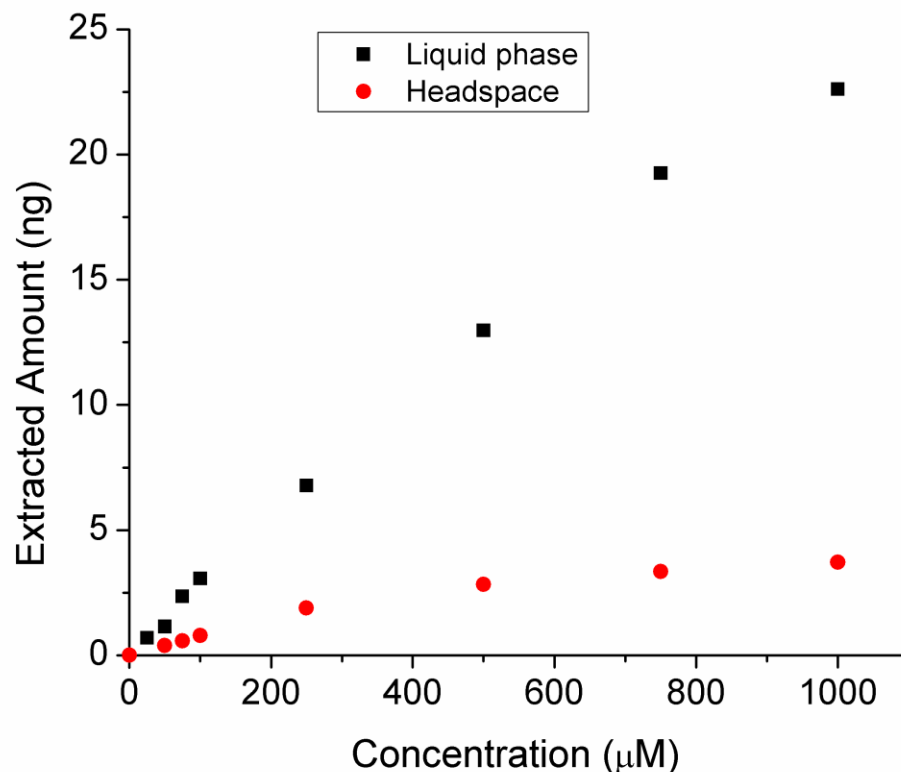


**Figure 4.6** Quinoline amount extracted in both liquid phase and headspace as a function of quinoline initial concentration.

For headspace extraction, a linear trend was found in the concentration range of 0 to 250  $\mu\text{M}$  with a correlation coefficient close to unity ( $R^2 = 0.9997$ ) and a slope of  $0.00761 \text{ ng}/\mu\text{M}$ . The detection limit was determined to be  $8.54 \mu\text{M}$  calculated by the standard deviation and the slope of the regression line. The proportional relationship between the extracted amount and the initial concentration can be described as the following equation for large sample volumes[6,7]:

$$n = [1 - \exp(-a \cdot t)] \cdot K_{fs} \cdot V_f \cdot C_0 \quad \text{Equation 4.11}$$

where  $n$  is the amount of analyte extracted,  $K_{fs}$  is the distribution coefficient of the analyte between the fiber coating and the sample matrix,  $V_f$  is the volume of extraction phase, and  $C_0$  is

the initial concentration of the analyte, which is quinoline in this case,  $t$  is the exposure time,  $a$  is a parameter measuring how fast partition equilibrium can be reached, which is a constant for a constantly agitated system. According to Equation (4.11), the amount of analyte extracted is proportional to the initial analyte concentration once the sampling time and agitation conditions are held constant, which is consistent with the results shown in Figure 4.6. Therefore, the quantitative analysis of SPME is feasible even before partition equilibrium is reached.

Both liquid phase direct extraction and headspace modes were feasible for quantitative analysis before equilibrium. The detection limit was lower in the headspace extraction than the liquid phase, which may be due to less matrix interference in the headspace mode. This led us to choose headspace mode for selectivity experiments. Thus coated fibers were exposed to the headspace of an aqueous solution containing 100  $\mu\text{M}$  quinoline and phenol in Tris buffer (pH = 8.0) for 2 minutes and analyzed by GC.

Compared to the PDMS fiber, which is a commonly used SPME fiber, the fluorinated receptor doped Teflon AF coating shows a higher selectivity of 11.1 compared to 3.8 for quinoline over phenol. The pure Teflon AF film also shows slightly higher selectivity (5.3 versus 3.8) than the pure PDMS film. Teflon AF 2400 has been found to contain one carboxylic acid group per 854 monomer units[100]. This may explain the slightly favored extraction of quinoline into the receptor-free Teflon AF film than PDMS. While the fiber-based selectivity using 50% (w/w) Krytox in Teflon AF coated fibers shows selectivity for quinoline (11.1), the selectivity is not as high as for the 96-well plate method (59). About a factor of two of this difference can be explained by the Henry's law constants of the analytes. Quinoline has a higher Henry's law constant (3700 mol/(kg\*bar)) compared to phenol (1900 mol/(kg\*bar))[101]. In addition, the 96-well vessel SPME experiments were carried out at equilibrium while the coated fiber SPME

experiments were performed before equilibrium to simplify and speed up the extraction process. Thus, we did a kinetic study for quinoline and phenol by a SPME fiber coated by Teflon AF with 50% Krytox as illustrated in Figure 4.7. The extracted amount of quinoline linearly increases with the exposure time while the extracted amount of phenol was almost zero due to no binding with the receptor. Further, the phenol amount extracted is at a plateau while the quinoline amount extracted is not. Thus, the selectivity actually increases when extraction time increases. This leads to a practical tradeoff – one can achieve high selectivity but at the cost of time.

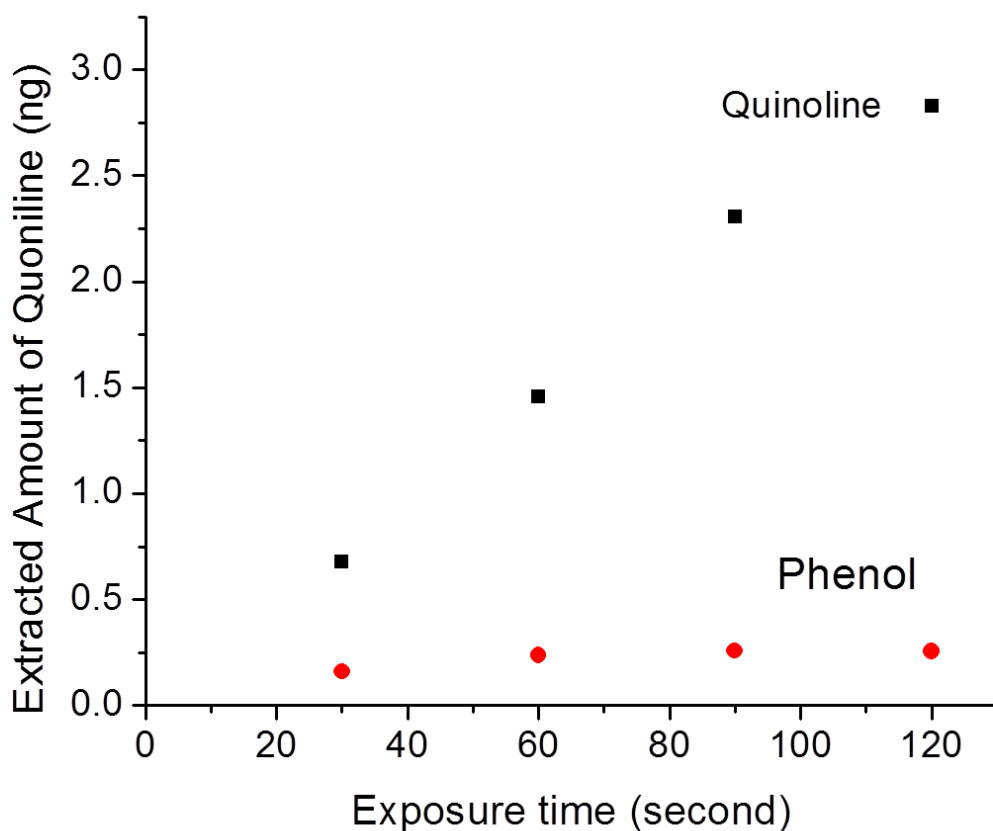


**Figure 4.7 Kinetic profile of extracted quinoline amount by the coated fiber (50% Krytox in Teflon AF) SPME-GC at different headspace exposure times.**

#### 4.4 CONCLUSIONS

We have demonstrated the distribution of a heterocyclic nitrogen-containing compound between Krytox 157 FSH doped Teflon AF 2400 films and buffered aqueous solution based on hydrogen bonding of the heterocyclic nitrogen group with the carboxylic acid group. We studied in both 96-well vessel SPME and the coated fiber SPME formats. The effects of receptor concentration and solute concentration on the extraction were studied. Those novel fluorinated SPME devices in both 96-well vessel format and the coated fiber design show selectivity for a heterocyclic nitrogen-containing compound compared to its non-heterocyclic counterpart. Those novel receptor-doped fluorinated SPME devices show great potential to detect quinoline-like potential environment pollutants in river water or other aqueous media.

## BIBLIOGRAPHY

- [1] T. Hyotylainen, M.-L. Riekkola, Sorbent- and liquid-phase microextraction techniques and membrane-assisted extraction in combination with gas chromatographic analysis: A review *Analytica Chimica Acta* 614 (2008) 27-37.
- [2] J. Pawliszyn, *Solid Phase Microextraction, Theory and Practice*, Wiley-VCH, New York, NY, 1997.
- [3] G. Ouyang, D. Vuckovic, J. Pawliszyn, Nondestructive Sampling of Living Systems Using in Vivo Solid-Phase Microextraction *Chemical Reviews* 111 (2011) 2784-2814.
- [4] C.L. Arthur, L.M. Killam, K.D. Buchholz, J. Pawliszyn, J.R. Berg, Automation and optimization of solid-phase microextraction *Analytical Chemistry* 64 (1992) 1960-1966.
- [5] G. Ouyang, J. Pawliszyn, Configurations and calibration methods for passive sampling techniques *Journal of Chromatography A* 1168 (2007) 226-235.
- [6] J. Ai, Headspace Solid Phase Microextraction. Dynamics and Quantitative Analysis before Reaching a Partition Equilibrium *Analytical Chemistry* 69 (1997) 3260-3266.
- [7] J. Ai, Solid Phase Microextraction for Quantitative Analysis in Nonequilibrium Situations *Analytical Chemistry* 69 (1997) 1230-1236.
- [8] J. Pawliszyn, *RSC Chromatography Monographs*, Royal Society of Chemistry, Letchworth, Hertfordshire, UK, 1999.
- [9] C. Dietz, J. Sanz, C. Camara, Recent developments in solid-phase microextraction coatings and related techniques *Journal of Chromatography A* 1103 (2006) 183-192.
- [10] J. Li, H. Chen, H. Chen, Y. Ye, Selective determination of trace thiamphenicol in milk and honey by molecularly imprinted polymer monolith microextraction and high-performance liquid chromatography *J. Sep. Sci.* 35 (2012) 137-144.
- [11] X. Hu, Q. Cai, Y. Fan, T. Ye, Y. Cao, C. Guo, Molecularly imprinted polymer coated solid-phase microextraction fibers for determination of Sudan I-IV dyes in hot chili powder and poultry feed samples *J. Chromatogr., A* 1219 (2012) 39-46.
- [12] M.A. Golsefid, Z. Es'haghi, A. Sarafraz-Yazdi, Design, synthesis and evaluation of a molecularly imprinted polymer for hollow fiber-solid phase microextraction of chlorogenic acid in medicinal plants *J. Chromatogr., A* 1229 (2012) 24-29.
- [13] D.-L. Deng, J.-Y. Zhang, C. Chen, X.-L. Hou, Y.-Y. Su, L. Wu, Monolithic molecular imprinted polymer fiber for recognition and solid phase microextraction of ephedrine and pseudoephedrine in biological samples prior to capillary electrophoresis analysis *J. Chromatogr., A* 1219 (2012) 195-200.
- [14] X. Hu, G. Dai, J. Huang, H. Jin, Y. Yu, Y. Liang, Preparation and Characterization of Metolachlor Molecularly Imprinted Polymer Coating on Stainless Steel Fibers for Solid-Phase Microextraction *Anal. Lett.* 44 (2011) 1358-1370.

- [15] F. Barahona, E. Turiel, A. Martin-Esteban, Supported liquid membrane-protected molecularly imprinted fibre for solid-phase microextraction of thiabendazole *Anal. Chim. Acta* 694 (2011) 83-89.
- [16] J. Zhou, C. Ma, S. Zhou, P. Ma, F. Chen, Y. Qi, H. Chen, Preparation, evaluation and application of molecularly imprinted solid-phase microextraction monolith for selective extraction of pirimicarb in tomato and pear *J. Chromatogr., A* 1217 (2010) 7478-7483.
- [17] L. Qiu, W. Liu, M. Huang, L. Zhang, Preparation and application of solid-phase microextraction fiber based on molecularly imprinted polymer for determination of anabolic steroids in complicated samples *J. Chromatogr., A* 1217 (2010) 7461-7470.
- [18] H. Zhang, A. Hussam, S.G. Weber, Properties and Transport Behavior of Perfluorotripentylamine (FC-70)-Doped Amorphous Teflon AF 2400 Films *Journal of the American Chemical Society* 132 (2010) 17867-17879.
- [19] X. Zhou, X. Shao, J.-j. Shu, M.-m. Liu, H.-l. Liu, X.-h. Feng, F. Liu, Thermally stable ionic liquid-based sol-gel coating for ultrasonic extraction-solid-phase microextraction-gas chromatography determination of phthalate esters in agricultural plastic films *Talanta* 89 (2012) 129-135.
- [20] C.M. Graham, Y.-J. Meng, T. Ho, J.L. Anderson, Sorbent coatings for solid-phase microextraction based on mixtures of polymeric ionic liquids *J. Sep. Sci.* 34 (2011) 340-346.
- [21] X. Zhou, P.-F. Xie, J. Wang, B.-B. Zhang, M.-M. Liu, H.-L. Liu, X.-H. Feng, Preparation and characterization of novel crown ether functionalized ionic liquid-based solid-phase microextraction coatings by sol-gel technology *J. Chromatogr., A* 1218 (2011) 3571-3580.
- [22] Y. Meng, V. Pino, J.L. Anderson, Role of counteranions in polymeric ionic liquid-based solid-phase microextraction coatings for the selective extraction of polar compounds *Anal. Chim. Acta* 687 (2011) 141-149.
- [23] Y. Meng, J.L. Anderson, Tuning the selectivity of polymeric ionic liquid sorbent coatings for the extraction of polycyclic aromatic hydrocarbons using solid-phase microextraction *J. Chromatogr., A* 1217 (2010) 6143-6152.
- [24] J. Huang, Y. Hu, Y. Hu, G. Li, Development of metal complex imprinted solid-phase microextraction fiber for 2,2'-dipyridine recognition in aqueous medium *Talanta* 83 (2011) 1721-1729.
- [25] Y. Sun, W.-Y. Zhang, J. Xing, C.-M. Wang, Solid-phase microfibers based on modified single-walled carbon nanotubes for extraction of chlorophenols and organochlorine pesticides *Microchim. Acta* 173 (2011) 223-229.
- [26] A. Sarafraz-Yazdi, A. Amiri, G. Rounaghi, H.E. Hosseini, A novel solid-phase microextraction using coated fiber based sol-gel technique using poly(ethylene glycol) grafted multi-walled carbon nanotubes for determination of benzene, toluene, ethylbenzene and o-xylene in water samples with gas chromatography-flame ionization detector *J. Chromatogr., A* 1218 (2011) 5757-5764.
- [27] C. Beining, S. Piletsky, A.P.F. Turner, Molecular Recognition: Design of "Keys" *Combinatorial Chemistry & High Throughput Screening* 5 (2002) 409.
- [28] S. Li, L. Sun, Y. Chung, S.G. Weber, Artificial Receptor-Facilitated Solid-Phase Microextraction of Barbiturates *Anal. Chem.* 71 (1999) 2146-2151.
- [29] S. Li, S.G. Weber, Determination of Barbiturates by Solid-Phase Microextraction and Capillary Electrophoresis *Analytical Chemistry* 69 (1997) 1217-1222.

- [30] G.R. Eldridge, H.C. Vervoort, C.M. Lee, P.A. Cremin, C.T. Williams, S.M. Hart, M.G. Goering, M. O'Neil-Johnson, L. Zeng, High-Throughput Method for the Production and Analysis of Large Natural Product Libraries for Drug Discovery *Analytical Chemistry* 74 (2002) 3963-3971.
- [31] J. O'Reilly, Q. Wang, L. Setkova, J.P. Hutchinson, Y. Chen, H.L. Lord, C.M. Linton, J. Pawliszyn, Automation of solid-phase microextraction *Journal of Separation Science* 28 (2005) 2010-2022.
- [32] R. Vatinno, D. Vuckovic, C.G. Zambonin, J. Pawliszyn, Automated high-throughput method using solid-phase microextraction-liquid chromatography-tandem mass spectrometry for the determination of ochratoxin A in human urine *Journal of Chromatography A* 1201 (2008) 215-221.
- [33] D. Vuckovic, E. Cudjoe, D. Hein, J. Pawliszyn, Automation of Solid-Phase Microextraction in High-Throughput Format and Applications to Drug Analysis *Analytical Chemistry* 80 (2008) 6870-6880.
- [34] E. Cudjoe, D. Vuckovic, D. Hein, J. Pawliszyn, Investigation of the Effect of the Extraction Phase Geometry on the Performance of Automated Solid-Phase Microextraction *Analytical Chemistry* 81 (2009) 4226-4232.
- [35] J.P. Hutchinson, L. Setkova, J. Pawliszyn, Automation of solid-phase microextraction on a 96-well plate format *Journal of Chromatography A* 1149 (2007) 127-137.
- [36] D. Vuckovic, E. Cudjoe, F.M. Musteata, J. Pawliszyn, Automated solid-phase microextraction and thin-film microextraction for high-throughput analysis of biological fluids and ligand-receptor binding studies *Nat. Protocols* 5 (2010) 140-161.
- [37] Mei-Fen Jeng, H.H. Dyson, Direct Measurement of the Aspartic Acid 26 pKa for Reduced Escherichia coli Thioredoxin by <sup>13</sup>C NMR *Biochemistry* 35 (1996) 1-6.
- [38] K. Box, C. Bevan, J. Comer, A. Hill, R. Allen, D. Reynolds, High-Throughput Measurement of pKa Values in a Mixed-Buffer Linear pH Gradient System *Analytical Chemistry* 75 (2003) 883-892.
- [39] R.I. Allen, K.J. Box, J.E.A. Comer, C. Peake, K.Y. Tam, Multiwavelength spectrophotometric determination of acid dissociation constants of ionizable drugs *Journal of Pharmaceutical and Biomedical Analysis* 17 (1998) 699-712.
- [40] S.K. Poole, C.F. Poole, Separation methods for estimating octanol-water partition coefficients *Journal of Chromatography, B: Analytical Technologies in the Biomedical and Life Sciences* 797 (2003) 3-19.
- [41] C. Foulon, N. Duhal, B. Lacroix-Callens, C. Vaccher, J.P. Bonte, J.F. Goossens, Determination of pKa values of benzoxa-, benzothia- and benzoselena-zolinone derivatives by capillary electrophoresis: Comparison with potentiometric titration and spectrometric data *European Journal of Pharmaceutical Sciences* 31 (2007) 165-171.
- [42] R. Collander, Partition of organic compounds between higher alcohols and water *Acta Chemica Scandinavica* 5 (1951) 774-780.
- [43] A. Leo, C. Hansch, D. Elkins, Partition coefficients and their uses *Chemical Reviews* (Washington, DC, United States) 71 (1971) 525-616.
- [44] M. Tachibana, M. Furusawa, N. Kiba, Application of solvent extraction and synchronous spectrofluorimetry to the determination of the formation constant for a 1:1 complex of carbazole with  $\beta$ -cyclodextrin in water-dimethyl sulfoxide medium *Journal of Inclusion Phenomena and Molecular Recognition in Chemistry* 22 (1995) 313-329.

- [45] L.-G.a. Danielsson, Y.-H. Zhang, Methods for determining n-octanol-water partition constants *TrAC Trends in Analytical Chemistry* 15 (1996) 188-196.
- [46] J. Sangster, *Octanol-water Partition Coefficients: Fundamentals and Physical Chemistry*, Wiley, New York, 1997.
- [47] OECD Guidelines for the Testing of Chemicals, Test No.117, OECD - Organisation for Economic Co-operation and Development, Paris, 2004.
- [48] Z. Chen, S.G. Weber, High-Throughput Method for Lipophilicity Measurement *Analytical Chemistry* 79 (2007) 1043-1049.
- [49] L. Hitzel, A.P. Watt, K.L. Locker, An Increased Throughput Method for the Determination of Partition Coefficients *Pharmaceutical Research* 17 (2000) 1389-1395.
- [50] T. Loftsson, D. Hreinsdottir, M. Masson, Evaluation of cyclodextrin solubilization of drugs *International journal of pharmaceutics* 302 (2005) 18-28.
- [51] T. Kennedy, Managing the drug discovery/development interface *Drug Discovery Today* 2 (1997) 436-444.
- [52] E. Ratti, & Trist, D., Continuing evolution of the drug discovery process in the pharmaceutical industry *Pure and Applied Chemistry* 73 (2001) 67-75.
- [53] A. Glomme, J. Marz, J.B. Dressman, comparison of a minaturized shake-flask solubility method with automated potentiometric acid/base titration and calculated solubilities *Journal of Pharmaceutical Sciences* 94 (2005) 1-16.
- [54] N.G. Das, S.K. Das, Formulation of poorly soluble drugs *Drug Delivery Report Spring/Summer* (2006) 52-55.
- [55] A.R. Hedges, Industrial applications of cyclodextrins *Chemical Reviews* (Washington, D. C.) 98 (1998) 2035-2044.
- [56] K. Uekama, F. Hirayama, T. Irie, Cyclodextrin Drug Carrier Systems *Chemical Reviews* (Washington, D. C.) 98 (1998) 2045-2076.
- [57] T. Loftsson, M.E. Brewster, M. Masson, Role of cyclodextrins in improving oral drug delivery *American Journal of Drug Delivery* 2 (2004) 261-275.
- [58] W. Hirsch, V. Fried, L. Altman, Effect of cyclodextrins on sparingly soluble salts *Journal of Pharmaceutical Sciences* 74 (1985) 1123-1125.
- [59] N. Bodor, P. Buchwald, Theoretical insights into the formation, structure, and energetics of some cyclodextrin complexes *Journal of Inclusion Phenomena and Macrocyclic Chemistry* 44 (2003) 9-14.
- [60] V.M. Rao, V.J. Stella, When can cyclodextrins be considered for solubilization purposes? *Journal of Pharmaceutical Sciences* 92 (2003) 927-932.
- [61] T. Higuchi, K.A. Connors, Phase-solubility techniques *Advan. Anal. Chem. Instr.* 4 (1965) 117-212.
- [62] M. Masson, B.V. Sigurdardottir, K. Matthiasson, T. Loftsson, Investigation of drug-cyclodextrin complexes by a phase-distribution method: Some theoretical and practical considerations *Chemical & Pharmaceutical Bulletin* 53 (2005) 958-964.
- [63] W. Eli, W. Chen, Q. Xue, Determination of association constants of cyclodextrin-nonionic surfactant inclusion complexes by a partition coefficient method *Journal of Inclusion Phenomena and Macrocyclic Chemistry* 38 (2000) 37-43.
- [64] Z. Chen, Y. Yang, S. Werner, P. Wipf, S.G. Weber, A screening method for chiral selectors that does not require covalent attachment *Journal of the American Chemical Society* 128 (2006) 2208-2209.

- [65] P. Mura, M.T. Faucci, A. Manderioli, G. Bramanti, Multicomponent systems of econazole with hydroxyacids and cyclodextrins *Journal of Inclusion Phenomena and Macrocyclic Chemistry* 39 (2001) 131-138.
- [66] Y.C. Guillaume, E. Peyrin, Symmetry Breaking during the Formation of  $\beta$ -Cyclodextrin-Imidazole Inclusion Compounds: Capillary Electrophoresis Study *Analytical Chemistry* 71 (1999) 2046-2052.
- [67] M. Pedersen, S. Bjerregaard, J. Jacobsen, A. Rommelmayer Larsen, A. Mehlsen Sorensen, An econazole  $\beta$ -cyclodextrin inclusion complex: an unusual dissolution rate, supersaturation, and biological efficacy example *International journal of pharmaceutics* 165 (1998) 57-68.
- [68] M. Pedersen, Isolation and antimycotic effect of a genuine miconazole- $\beta$ -cyclodextrin complex *European Journal of Pharmaceutics and Biopharmaceutics* 40 (1994) 19-23.
- [69] M.I. El-Barghouthi, N.A. Masoud, J.K. Al-Kafawein, A.A. Abdoh, Inclusion complexation of itraconazole with  $\beta$ - and 2-hydroxypropyl- $\beta$ -cyclodextrins in aqueous solutions *Russian Journal of Physical Chemistry* 80 (2006) 1050-1055.
- [70] J. Peeters, P. Neeskens, J.P. Tollenaere, P. Van Remoortere, M.E. Brewster, Characterization of the interaction of 2-hydroxypropyl- $\beta$ -cyclodextrin with itraconazole at pH 2, 4, and 7 *Journal of Pharmaceutical Sciences* 91 (2002) 1414-1422.
- [71] K. Miyake, T. Irie, H. Arima, F. Hirayama, K. Uekama, M. Hirano, Y. Okamaoto, Characterization of itraconazole/2-hydroxypropyl- $\beta$ -cyclodextrin inclusion complex in aqueous propylene glycol solution *International journal of pharmaceutics* 179 (1999) 237-245.
- [72] M. Pedersen, M. Edelsten, V.F. Nielsen, A. Scarpellini, S. Skytte, C. Slot, Formation and antimycotic effect of cyclodextrin inclusion complexes of econazole and miconazole *International journal of pharmaceutics* 90 (1993) 247-254.
- [73] I. Shehatta, A.H. Al-Marzouqi, B. Jobe, A. Dowaidar, Enhancement of aqueous solubility of itraconazole by complexation with cyclodextrins using supercritical carbon dioxide *Canadian Journal of Chemistry* 83 (2005) 1833-1838.
- [74] OECD guidelines for the testing of chemicals, No.107, Partition coefficient (n-octanol/water): Shake Flask Method, Organization for Economic Co-operation and Development (OECD), Paris, 1995.
- [75] K. Carlsson, B. Karlberg, Determination of octanol-water partition coefficients using a micro-volume liquid-liquid flow extraction system *Anal. Chim. Acta* 423 (2000) 137-144.
- [76] L. Hitzel, A.P. Watt, K.L. Locker, An increased throughput method for the determination of partition coefficients *Pharm. Res.* 17 (2000) 1389-1395.
- [77] OECD guidelines for the testing of chemicals No.117: Partition coefficient (n-octanol/water), High Performance Liquid Chromatography (HPLC) Method, Organization for Economic Co-operation and Development (OECD), Paris, 2004.
- [78] M. Kah, C. Brown, LogD: liphilicity for ionisable compounds *Chemosphere* 72 (2008) 1401-1408.
- [79] E.H. Kerns, L. Di, Drug-like properties : concepts, structure design and methods : from ADME to toxicity optimization, Academic Press, Amsterdam ; Boston, 2008.
- [80] Z. Chen, D. Lu, S.G. Weber, High-throughput phase-distribution method to determine drug-cyclodextrin binding constants *Journal of Pharmaceutical Sciences* 98 (2009) 229-238.

- [81] H. Abe, M. Tanaka, K. Sugimoto, A. Suma, M. Yokota, S. M, K. Lio, K. Ueyama, D. Motoda, T. Noguchi, T. Adachi, J. Tsuruha, S. Doi, Preparation of piperazine derivatives as hepatitis C virus (HCV) polymerase inhibitors, Japan Tobacco Inc., Japan, 2007.
- [82] Anna Maria Almerico, Antonino Lauria, Marco Tutone, Patrizia Diana, Paola Barraja , Alessandra Montalbano , Girolamo Cirrincione , G. Dattolo, A Multivariate Analysis on Non-nucleoside HIV-1 Reverse Transcriptase Inhibitors and Resistance Induced by Mutation QSAR & Combinatorial Science 22 (2003) 984-996.
- [83] A. Giraldez, R. Nieves, C. Ochoa, C. Vara de Rey, E. Cenarruzabeitia, B. Lasheras, Analgesic and antipyretic activities of 1,2,6-thiadiazin-3-one 1,1-dioxides. SAR design of a new analgesic agent European Journal of Medicinal Chemistry 24 (1989) 497-502.
- [84] A. Castro, A. Martinez, I. Cardelus, J. Llenas, Dioxides of bicyclic thiadiazines: a new family of smooth muscle relaxants Bioorganic & Medicinal Chemistry 3 (1995) 179-185.
- [85] C.A.L. Lipinski, F.; Dominy, B. W.; Feeney, P. J., Advanced Drug Delivery Reviews 23 (1997) 3-25.
- [86] C.A. Lipinski, Drug-like properties and the causes of poor solubility and poor permeability Journal of Pharmacological and Toxicological Methods 44 (2001) 235-249.
- [87] S. Li, L. Sun, Y. Chung, S.G. Weber, Artificial Receptor-Facilitated Solid-Phase Microextraction of Barbiturates Analytical Chemistry 71 (1999) 2146-2151.
- [88] J.A. Gladysz, D.P. Curran, I.T. Horvath, Handbook of Fluorous Chemistry, Wiley-VCH, Weinheim, Germany, 2004.
- [89] J.-M. Vincent, Noncovalent associations in fluorous fluids Journal of Fluorine Chemistry 129 (2008) 903-909.
- [90] C. Palomo, J.M. Aizpurua, I. Loinaz, M.J. Fernandez-Berridi, L. Irusta, Scavenging of Fluorinated N,N'-Dialkylureas by Hydrogen Binding: A Novel Separation Method for Fluorous Synthesis Org. Lett. 3 (2001) 2361-2364.
- [91] K.L. O'Neal, S. Geib, S.G. Weber, Extraction of Pyridines into Fluorous Solvents Based on Hydrogen Bond Complex Formation with Carboxylic Acid Receptors Analytical Chemistry 79 (2007) 3117-3125.
- [92] A.Y. Alentiev, V.P. Shantarovich, T.C. Merkel, V.I. Bondar, B.D. Freeman, Y.P. Yampolskii, Gas and Vapor Sorption, Permeation, and Diffusion in Glassy Amorphous Teflon AF1600 Macromolecules 35 (2002) 9513-9522.
- [93] H. Zhang, S. Wang, S.G. Weber, Nanocomposite Teflon AF 2400 Films as Tunable Platforms for Selective Transport Analytical Chemistry 84 (2012) 9920-9927.
- [94] H. Zhao, K. Ismail, S.G. Weber, How Fluorous Is Poly(2,2-bis(trifluoromethyl)-4,5-difluoro-1,3-dioxane-co-tetrafluoroethylene) (Teflon AF)? Journal of the American Chemical Society 126 (2004) 13184-13185.
- [95] H. Zhao, J. Zhang, N. Wu, X. Zhang, K. Crowley, S.G. Weber, Transport of Organic Solutes through Amorphous Teflon AF Films Journal of the American Chemical Society 127 (2005) 15112-15119.
- [96] D. Lu, P. Chambers, P. Wipf, X.-Q. Xie, D. Englert, S. Weber, Lipophilicity screening of novel drug-like compounds and comparison to clog *P* Journal of Chromatography A 1258 (2012) 161-167.
- [97] Toxicological Review of Quinoline, USEPA, Washington, DC, 2001.
- [98] K.L. O'Neal, S.G. Weber, Molecular and ionic hydrogen bond formation in fluorous solvents J Phys Chem B 113 (2009) 149-158.

- [99] OSHA, Occupational Safety and Health Guideline for Phenol, Occupational Safety and Health Administration, Washington DC, 1996.
- [100] C.-Z. Lai, S.S. Koseoglu, E.C. Lugert, P.G. Boswell, J. Rábai, T.P. Lodge, P. Bühlmann, Fluorous Polymeric Membranes for Ionophore-Based Ion-Selective Potentiometry: How Inert Is Teflon AF? *Journal of the American Chemical Society* 131 (2009) 1598-1606.
- [101] Air and steam stripping of toxic pollutants, USEPA, Cincinnati, OH, USA, 1982.